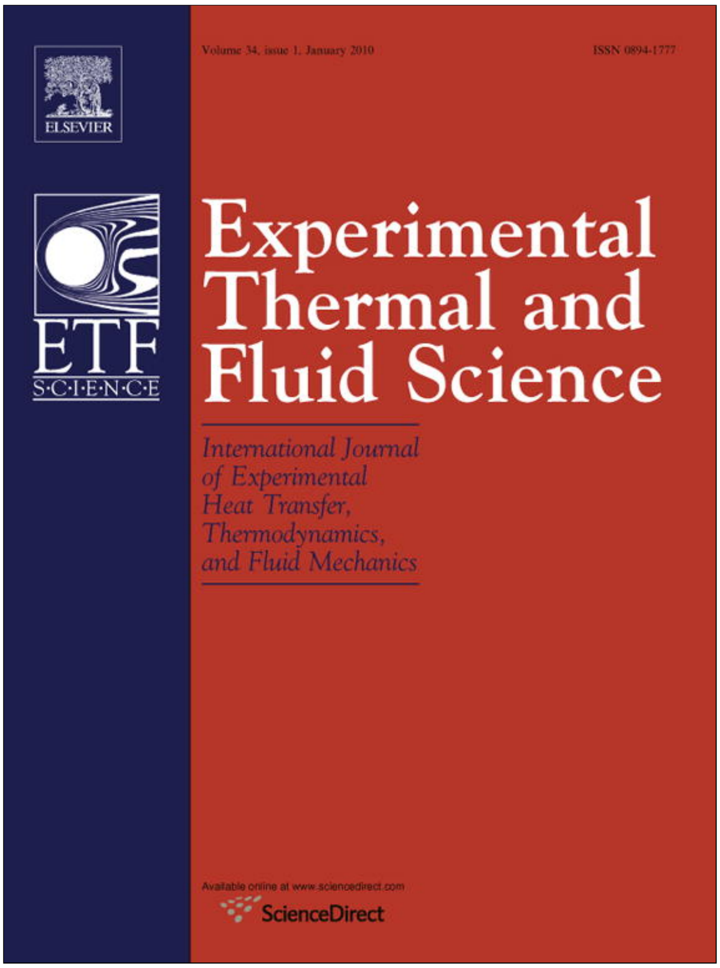
Volume 34, issue 1, January 2010
ISSN 0894-1777
ELSEVIER
ETF
S·C·I·E·N·C·E
Experimental Thermal and Fluid Science
International Journal of Experimental Heat Transfer, Thermodynamics, and Fluid Mechanics
Available online at www.sciencedirect.com
ScienceDirect

Experimental Thermal and Fluid Science 34 (2010) 53–62

Contents lists available at ScienceDirect

Experimental Thermal and Fluid Science

journal homepage: www.elsevier.com/locate/etfs

Turbulent heat transfer enhancement by counter/co-swirling flow in a tube fitted with twin twisted tapes

S. Eiamsa-ard [a,*], C. Thianpong [b], P. Eiamsa-ard [b]

[a] Department of Mechanical Engineering, Faculty of Engineering, Mahanakorn University of Technology, Bangkok 10530, Thailand
[b] Department of Mechanical Engineering, Faculty of Engineering, King Mongkut's Institute of Technology Ladkrabang, Bangkok 10520, Thailand

ARTICLE INFO

Article history:
Received 17 April 2009
Received in revised form 20 August 2009
Accepted 7 September 2009

Keywords:
Heat transfer
Friction factor
Enhancement index
Twin counter twisted tapes
Twin co-twisted tapes

ABSTRACT

In the present study, the influences of twin-counter/co-twisted tapes (*counter/co-swirl tape*) on heat transfer rate (*Nu*), friction factor (*f*) and thermal enhancement index (η) are experimentally determined. The twin counter twisted tapes (*CTs*) are used as *counter-swirl flow generators* while twin co-twisted tapes (*CoTs*) are used as *co-swirl flow generators* in a test section. The tests are conducted using the *CTs* and *CoTs* with four different twist ratios (y/w = 2.5, 3.0, 3.5 and 4.0) for Reynolds numbers range between 3700 and 21,000 under uniform heat flux conditions. The experiments using the single twisted tape (*ST*) are also performed under similar operation test conditions, for comparison. The experimental results demonstrate that Nusselt number (*Nu*), friction factor (*f*) and thermal enhancement index (η) increase with decreasing twist ratio (y/w). The results also show that the *CTs* are more efficient than the *CoTs* for heat transfer enhancement. In the range of the present work, heat transfer rates in the tube fitted with the *CTs* are around 12.5–44.5% and 17.8–50% higher than those with the *CoTs* and *ST*, respectively. The maximum thermal enhancement indices (η) obtained at the constant pumping power by the *CTs* with y/w = 2.5, 3.0, 3.5 and 4.0, are 1.39, 1.24, 1.12 and 1.03, respectively, while those obtained by using the *CoTs* with the same range of y/w are 1.1, 1.03, 0.97 and 0.92, respectively. In addition, the empirical correlations of the heat transfer (*Nu*), friction factor (*f*) and thermal enhancement index (η) are also reported.

1. Introduction

A high cost of energy and material has resulted in an increased effort aimed at producing more efficient heat exchange equipment. The methods of improving convective heat transfer in the tubes of heat exchangers have been widely investigated by many researchers. Heat transfer enhancement techniques can be classified into two groups: (1) active technique that needs external power source and (2) passive technique which does not need external power source. Both active and passive techniques have been applied to improve heat transfer in several areas such as nuclear reactors, chemical reactors and general heat exchangers. The principle of the passive technique involves either surface treatment, such as coated surface, rough surface and extended surface or flow manipulation such as swirl flow and modified flow. One of the most favourable passive techniques is generating swirl flow by insertion of a twisted tape because the tape is inexpensive and can be easily employed to the existing system. The effects of twisted tape insertion have been widely studied for both experimental and numerical simulation works. The presence of twisted tape directs toward reducing the hydrodynamic or thermal boundary layer thickness, leading to greater convective heat transfer. However, in the process, pumping power may increase significantly and ultimately the pumping cost becomes high. Therefore, to achieve a desired heat transfer rate in an existing heat exchanger at an economic pumping power, the design of twisted tape with a proper geometry is necessary.

For several years, research work on heat transfer enhancement in heat exchanger by using twisted tape has grown strongly. After the success of the use of twisted tape for heat transfer augmentation which was early reported by Whitham [1], further improvements of thermal performance for tubes with various geometries of twisted tape inserts have been released. Kidd [2] and Klepper [3] invented the short length twisted tapes for the use in gas cooled nuclear reactor and inferred that the tapes were more efficient than the full length twisted tapes. Saha et al. [4] examined the heat transfer enhancement in a round tube fitted with the regularly spaced twisted tape elements. Date and Gaitonde [5] developed correlations for predicting characteristics of laminar flow in a tube fitted with regularly spaced twisted tape elements. In addition, the experimental investigations of heat transfer enhancement by means of regularly spaced twisted tapes were also reported by Dasmahapatra and Raja Rao [6] and Eiamsa-ard et al. [7].

* Corresponding author. Tel./fax: +66 2 9883666.
E-mail address: smith@mut.ac.th (S. Eiamsa-ard).

0894-1777/$ - see front matter © 2009 Elsevier Inc. All rights reserved.
doi:10.1016/j.expthermflusci.2009.09.002

Nomenclature

A	heat transfer surface area, m^2
C_p	specific heat at constant pressure, $J\ kg^{-1}\ K^{-1}$
D	inside diameter of the test tube, m
f	friction factor = $\Delta P/((L/D)(\rho U^2/2))$
h	heat transfer coefficient, $W\ m^{-2}\ K^{-1}$
I	current, A
k	thermal conductivity of fluid, $W\ m^{-1}\ K^{-1}$
L	length of the test section, m
M	mass flow rate, $kg\ s^{-1}$
Nu	Nusselt number = hD/k
P	pressure of flow in stationary tube, Pa
Pr	Prandtl number = $\mu C_p/k$
ΔP	pressure drop, Pa
Q	heat transfer rate, W
Re	Reynolds number = $\rho UD/\mu$
t	thickness of the test tube, m
T	temperature, °C
$\tilde{T}$	mean temperature, °C
U	average axial flow velocity, $m\ s^{-1}$
V	voltage, V
$\dot{V}$	volume flow rate, $m^3\ s^{-1}$
w	tape width, m
y	tape pitch length, m
y/w	twist ratio

Greek letters

δ	tape thickness, m
ρ	fluid density, $kg\ m^{-3}$
μ	fluid dynamic viscosity, $kg\ s^{-1}\ m^{-1}$
η	thermal enhancement index

Subscripts

b	bulk
conv	convection
e	empty tube
in	inlet
out	outlet
pp	pumping power
s	swirl generator
w	tube wall

Abbreviations

CTs	twin counter twisted tapes
CoTs	twin co-twisted tapes
ST	single twisted tape

A comparative study of heat transfer and friction factor in the round tubes fitted with single, twin and triple twisted tapes was reported by Chang et al. [8]. For their findings, the heat transfer enhancements achieved for laminar flows in the tubes fitted with single, twin and triple twisted tapes were, respectively, 1.5–2.3, 1.98–2.8 and 2.86–3.76 times of the Dittus–Boelter levels. In the range of $3000 < Re < 14{,}000$, the tubes fitted with twin and triple twisted tapes could offer the higher values of heat transfer augmentation with the similar levels of performance factor as those found in the tube fitted with single twisted tape. Chang et al. [9,10] also presented the promise of using the serrated twisted tapes and broken twisted tapes as heat transfer enhancing devices. As found, the heat transfer rates in the tubes fitted with the serrated and broken twisted tapes were, respectively, 1.25–1.67 and 1.28–2.4 times of that in the tube fitted with typical twisted tape. A recent study by Rahimi et al. [11] addressed the heat transfer, friction factor and thermal performance of a tube fitted with jagged, notched, perforated and classic twisted tapes for both experimental and computational fluid dynamics (CFD) works. Their results showed that the jagged twisted tape yielded higher heat transfer rate than the others. Bharadwaj et al. [12] determined the pressure drop and heat transfer behaviours in a 75-start spirally grooved tube fitted with twisted tape under laminar and moderately turbulent regions. They found that the direction of twist to grooved surface (clockwise and anticlockwise) influenced the thermo-hydraulic characteristics. Jaisankar et al. [13] investigated the heat transfer and friction factor characteristics of thermosyphon solar water heater system with full length twist tape, twist tape fitted with rod and spacer fitted at the trailing edge. It was observed that the overall performance for the twist tape fitted with rod was greater than that for the twist tape fitted with spacer. Apart from above literature review, literature of over hundred papers of heat transfer enhancement by using twisted tapes was described by Dewan et al. [14].

In the present work, twisted tapes with new design, twin-counter/co-twisted tapes (*counter/co-swirl tape*) are proposed for heat transfer enhancement in a circular tube. In the experiments, the twin counter twisted tapes (*CTs*) are used as the *counter-swirl flow generators* while the twin co-twisted tapes (*CoTs*) are used as *co-swirl flow generators*. The results obtained by the use of the newly designed twisted tapes are also compared with those by the use of the single twisted tape (*ST*) and the empty tube.

2. Twisted tapes

Twin twisted tapes are made of aluminium and have tape width (w) of 9 mm, tape thickness (δ) of 0.8 mm. and tape length (l) of 1000 mm. Dimensions of single twisted tape are same as those of the twin tapes, except tape width of 19 mm. Both twin-counter/co-twisted tapes were prepared with four different twist ratios, y/w = 2.5, 3.0, 3.5 and 4.0 where twist ratio is defined as twist length (180°/twist length) to tape width (w). The single tapes (*ST*) were prepared with three twist ratios, y/w = 3.0, 3.5 and 4.0, for comparative investigation. Comparison of geometric details of the twin-counter/co-twisted tapes (*counter/co-swirl tapes*) and also a single twisted tape is shown in Fig. 1 while details of tape geometries are presented in Table 1. The tape thickness of 0.8 mm was chosen to avoid tape twisting difficulty of the thinner tape which was torn easily during the twisting operation. On the other hand, to avoid an additional friction in the system that might be caused the thicker tape. To produce the twisted tape, one end of a straight tape was clamped while another end was carefully twisted to ensure a desired twist length. For twin twisted tapes, two tapes were twisted separately and then welded together with a small aluminium wire. As shown in Fig. 1, for the twin co-twisted tapes (*CoTs*), both tapes were well aligned and positioned to be twisted in same direction to generate identical direction swirl called *co-swirl flow*. On the other hand, the twin counter twisted tapes (*CTs*), two tapes were aligned to be twisted in opposite directions to produce *counter-swirl flow*.

3. Experimental setup

The experiments were carried out using an experimental facility as shown in Fig. 2. The test tube is made of copper and has inner diameter of 19 mm (D), outside diameter of 21 mm (D_o), wall thickness of 1.5 mm (t) and length of 1000 mm (L). In the experi-

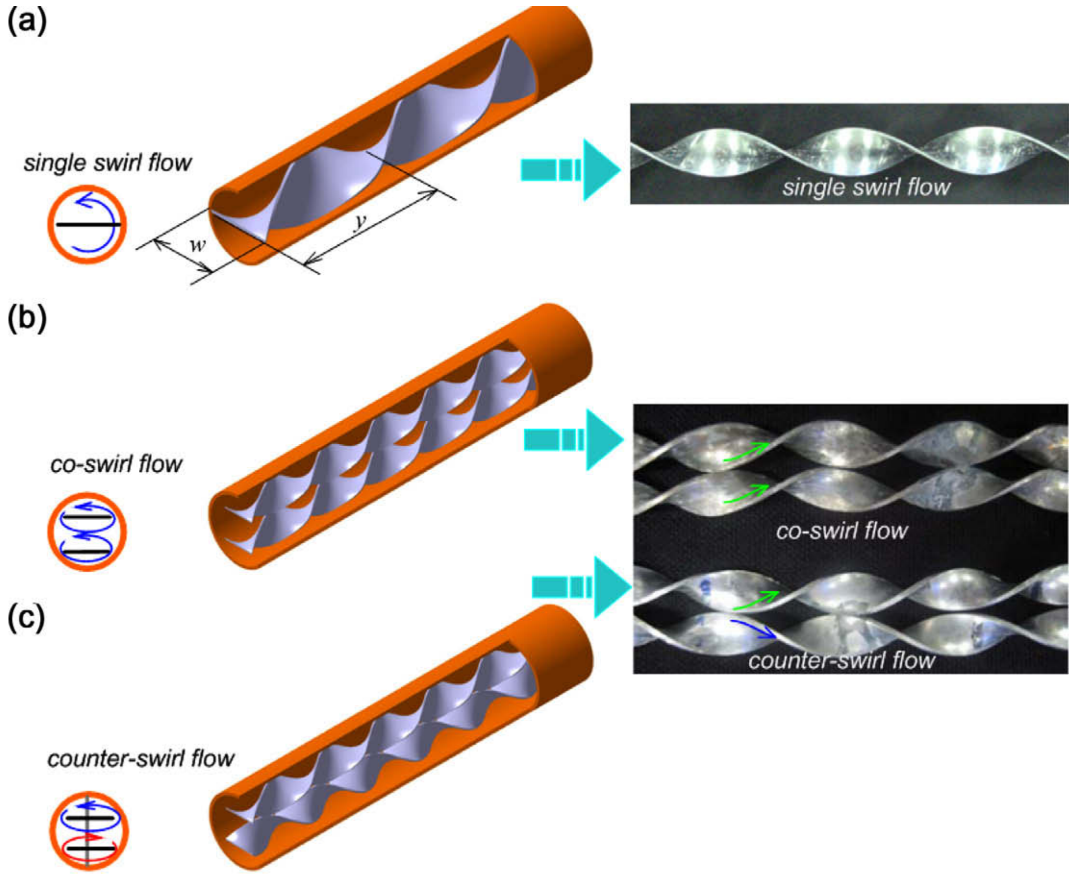

Fig. 1. Test tube with twisted tape inserts: (a) single twisted tape (*ST*), (b) twin co-twisted tapes (*CoTs*) and (c) twin counter twisted tapes (*CTs*).

Table 1
Details of twisted tape insert.

Twisted tape	*ST*	*CTs*	*CoTs*
(a) Tape width (w)	19 mm	9 mm	Same as *CTs*
(b) Tape pitch length (y)	57, 66.5 and 76 mm	22.5, 27, 31.5 and 36 mm	Same as *CTs*
(c) Twist ratio (y/w)	3.0, 3.5 and 4.0	2.5, 3.0, 3.5 and 4.0	Same as *CTs*
(d) Tape thickness (δ)	0.8 mm	Same as *ST*	Same as *ST*
(e) Material	Aluminium	Same as *ST*	Same as *ST*
(f) Swirl type	Single swirl flow	Counter-swirl flow	Co-swirl flow

ments, the single and twin-counter/co-twisted tapes were inserted at the core tube along the test section. The rather long tube provided sufficient contact surface between the tapes and tube wall for the firm attachment of the tapes to the tube without the need of any extra fitting. The tube was wound with electrical heating wire covered with ceramic beads. During the test, the tube was heated by continually winding flexible electrical wire providing a uniform heat flux condition. The electrical output power was controlled by a variac transformer to obtain a constant heat flux along the entire length of the test section and by keeping the current of less than 10 A. The outer surface of the test tube was well insulated to minimize convective heat leak to surroundings. Moreover, necessary precautions were taken to prevent leakages from the system. In the experiment, the heat transfer losses from the test tube are around 3–5% of the total heat input ($Q = IV$). The inner and outer temperatures of the water were measured at certain points with a multi-channel temperature measurement unit in conjunction with the resistance temperature detectors (RTDs). Fifteen thermocouples were tapped on the local wall of the tube and the thermocouples were placed round the tube to measure the circumferential temperature variation, which was found to be negligible. The mean wall temperature was determined by means of calculations based on the reading of copper–constantan thermocouples.

The test loop consists of a water pump, data logger, pressure transmitter, thermocouple/RTD, rotameter and heat transfer test section as depicted in Fig. 2. In the apparatus setting above, the inlet water from a reservoir tank was discharged through the rotameter then the heat transfer test section. For each test run, it was necessary to record the data of temperature, volumetric flow rate and pressure drop of the bulk water at steady state conditions in which the inlet water temperature was maintained constant at 27 °C. The various characteristics of the flow friction and the Reynolds numbers were based on the bulk temperature. During the test, local wall temperature, inlet and outlet water temperatures, pressure drop across the test section and flow velocity were measured. The average Nusselt numbers were calculated and discussed where all fluid properties were determined at the overall bulk mean temperature. Details of the test conditions are shown in Table 2.

The Reynolds numbers of the cold water were varied from 3700 to 21,000. Uncertainties of measurements are estimated based on ANSI/ASME. The uncertainties of axial velocity, pressure and temperature are found to be within ±7%, ±5% and ±0.5%, respectively. In addition, the uncertainties of non-dimensional parameters are ±5% for Reynolds number, ±10% for Nusselt number and ±12% for friction.

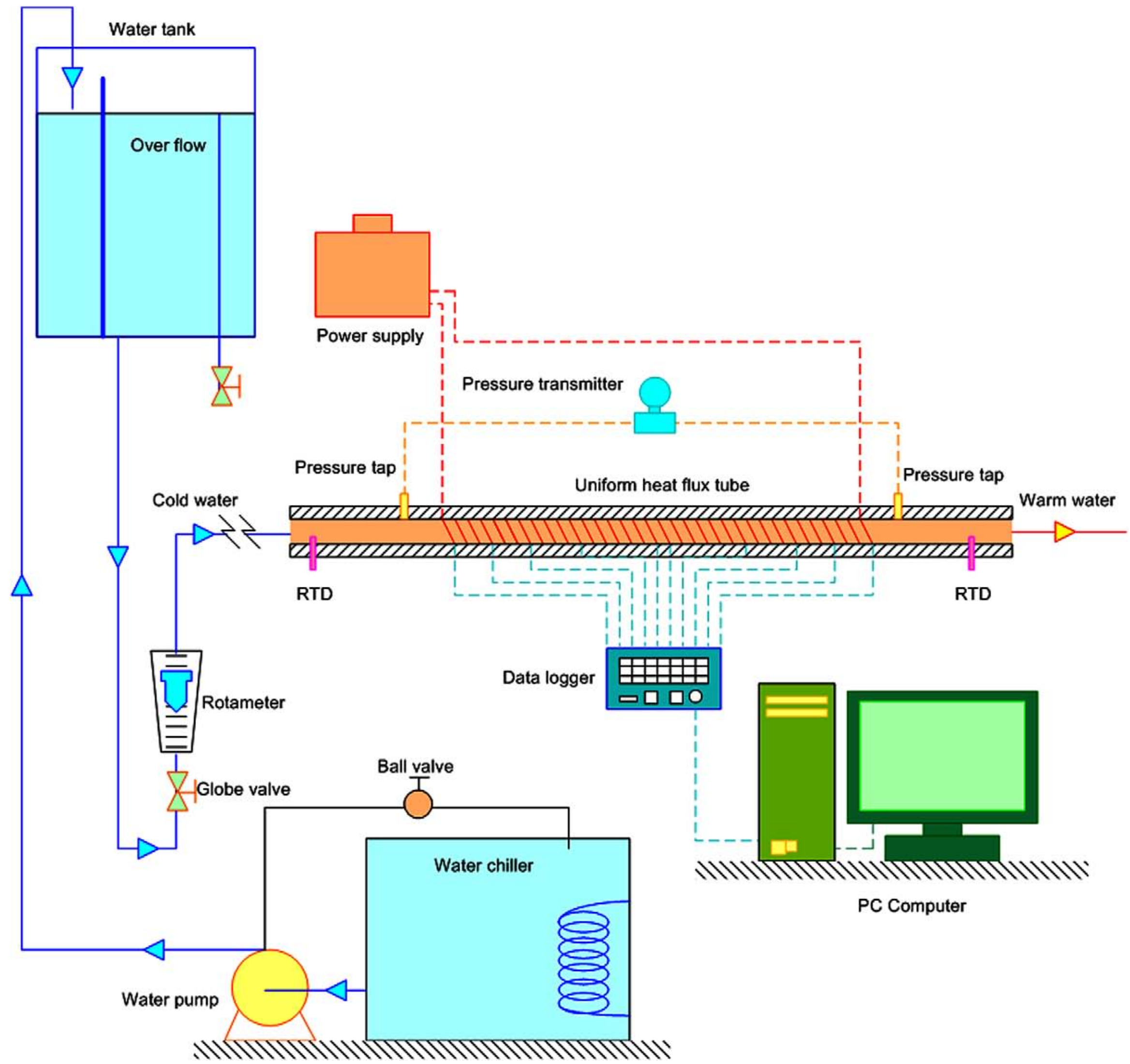

Fig. 2. Schematic diagram of the experimental heat transfer set-up.

Table 2
Details of heating tube and experimental conditions.

(a) Inner diameter	19 mm
(b) Outer diameter	21 mm
(c) Wall thickness	1.5 mm
(d) Length	1000 mm
(e) Material	Copper
(f) Wall condition	Uniform heat flux
(g) Reynolds number	3700–21,000
(h) Working fluid	Water

4. Heat transfer and friction factor measurements

In experiments, water is used as a working fluid and flowed through a test tube under uniform heat flux condition. The heat transfer rate at steady state is assumed to be equal to the heat loss from the test section which may be expressed as:

$$Q_{water} = Q_{conv} \tag{1}$$

Then the heat transferred from the water flow can be drawn as,

$$Q_{water} = MC_p(T_{out} - T_{in}) \tag{2}$$

The heat transferred from the tube wall by convection may be also written as,

$$Q_{conv} = hA\left|\widetilde{T}_w - \left(\frac{T_{out} + T_{in}}{2}\right)\right| \tag{3}$$

where T_{out} is the outlet temperature of water flow, T_{in} is the inlet water temperature, T_w is the temperature of the locations in the centerline of the tube wall and A is the total surface area of the inside tube wall, which can be expressed as:

$$A = \pi DL \tag{4}$$

where D is the inner diameter of the test tube. The average heat transfer coefficient (h) for the test tube can be calculated by the combination of Eqs. (2) and (3),

$$h = \frac{MC_p(T_{out} - T_{in})}{A\left|\widetilde{T}_w - \left(\frac{T_{out}+T_{in}}{2}\right)\right|} \tag{5}$$

In the experimental results, the average Nusselt number is defined as follow,

$$Nu = \frac{hD}{k} \quad (6)$$

where k is the local thermal conductivity of the fluid which calculated from the fluid properties at the local mean bulk fluid temperature ($T_b = (T_{out} + T_{in})/2$). The friction factor for tube with or without twisted tape can be calculated using pressure loss, ΔP, across the test length, L, via following equation:

$$f = \frac{1}{2}\frac{\Delta P}{L}\frac{D}{\rho U^2} \quad (7)$$

where ρ is the density at the mean bulk temperature, and U is the average velocity based on the inner diameter.

The Nusselt number, Prantl number, Reynolds number, and all of thermo-physical properties of the fluid were calculated of the basis of water properties corresponding to the bulk fluid temperature (T_b). The Reynolds number based on the total flow rate at the inlet of the test section is expressed as:

$$Re = \rho UD/\mu \quad (8)$$

where μ is the dynamic viscosity of the working fluid.

It is very important to validate the present empty tube data of Nusselt number and friction factor in fully developed straight/axial flow with the correlations from the previous studies. In the present work, Nusselt number and friction factor from the experimental data are compared with the correlations recommended by Dittus–Boelter and Blasius [15].

5. Experimental results

In this section, the heat transfer and friction factor characteristics and also thermal enhancement index in a tube fitted with twin-counter/co-twisted tapes (*counter/co-swirl tape*) are presented. The experiments are performed using twin twisted tapes with four different twist ratios, $y/w = 2.5$, 3.0, 3.5 and 4.0, in the range of Reynolds number between 3700 and 21,000. The results obtained for the tube fitted with the single twisted tapes (*ST*) with three different twist ratios, $y/w = 3.0$, 3.5 and 4.0, and the empty tube are used as the reference data for the performance evaluation of the modified twisted tapes.

5.1. Validation test

Empty tube data serve as a qualification for the facility and the procedure used over the range of Reynolds number studied. Qualification of the heat transfer rate (Nu) and friction factor (f) of the empty tube is evaluated by comparing the experimental data with the previous correlations [15] under similar conditions. The results shown in Fig. 3a and b, reveal that the data for present empty tube are in good agreement with the previous reports for both the Nusselt number (Nu) and the friction factor (f) correlations. As found, the mean absolute percentage deviations of the present experimental Nusselt number data are ±6% from the values predicted by Dittus–Boelter correlation, while the average absolute percentage deviations for friction factor data are ±10.4% from the values predicted by Blasius correlation. The empirical correlations of the Nusselt number and friction factor for the present empty tube can be expressed as follows:

$$Nu = 0.04Re^{0.75}Pr^{0.4} \quad (9)$$

$$f = 0.376Re^{-0.259} \quad (10)$$

Comparisons between the present results and correlations by Manglik and Bergles [16] using the tube fitted with single twisted tapes (*ST*) at three different twist ratios, $y/w = 3.0$, 3.5 and 4.0 are demonstrated in Fig. 4a and b for Nusselt number and Fig. 5a and b for friction factor. Compared to the results obtained from the past investigation [16], the present Nusselt numbers are found to be slightly lower while the present friction factors are noticeably higher at the low Reynolds number region and then become comparable at the high Reynolds number. In addition, it is obvious that the present Nusselt numbers and friction factors agree well with the available correlations within ±15–20% for both Nusselt number and friction factor.

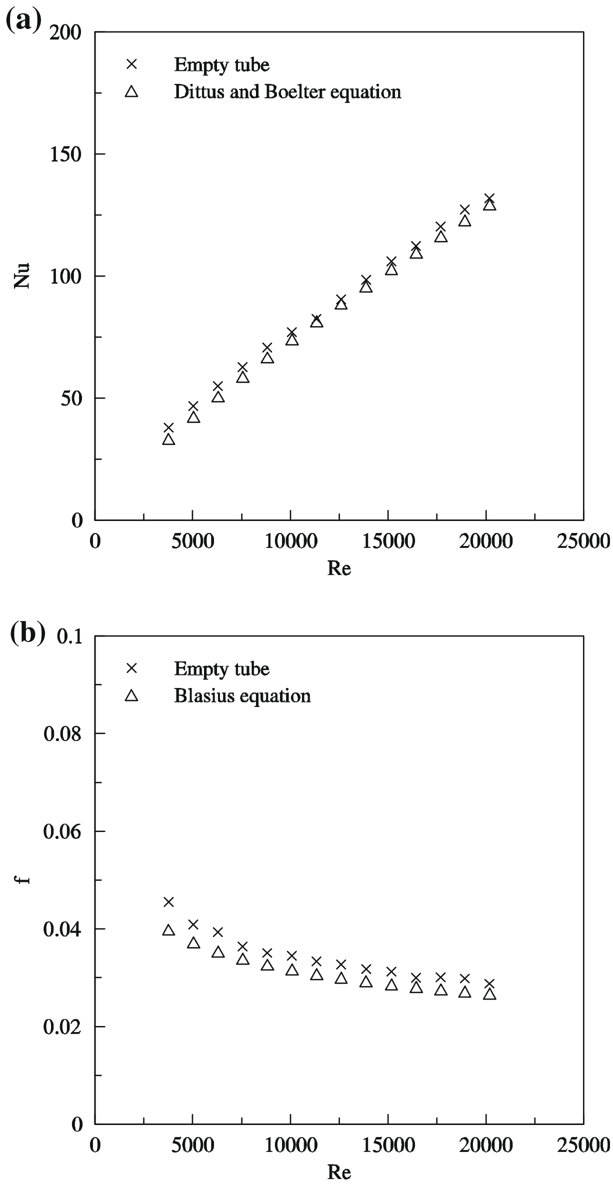

Fig. 3. Confirmatory test of empty tube: (a) Nusselt number and (b) friction factor.

5.2. Effect of twin-counter/co-twisted tape inserts

Effects of the twin counter twisted tapes (*CTs: counter-swirl flow generators*) and the twin co-twisted tapes (*CoTs: co-swirl flow generators*) on the heat transfer rate in a uniform heat flux tube are shown in Fig. 6. The results obtained for the tube fitted with the single twisted tape (*ST*), and the empty tube are also plotted for comparison. General trend found in Fig. 6 is that, the Nusselt number increases with the rise of Reynolds number. The influence for applying the *CTs* on heat transfer rate is significant for all Reynolds numbers.

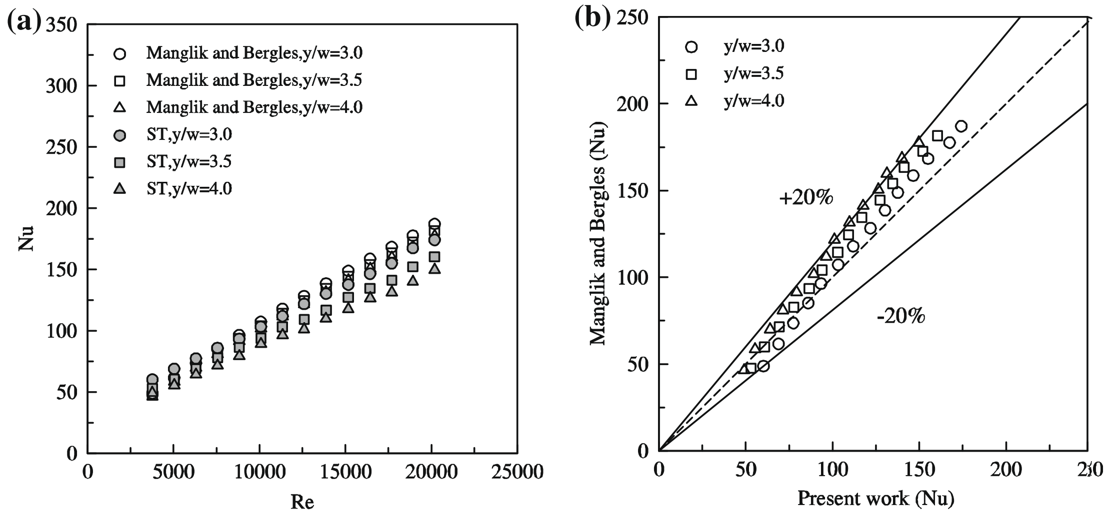

Fig. 4. Confirmatory test of Nusselt number of single twisted tape: (a) *Nu* and *Re* and (b) deviation of the present *Nu* from those by Manglik and Bergles [16].

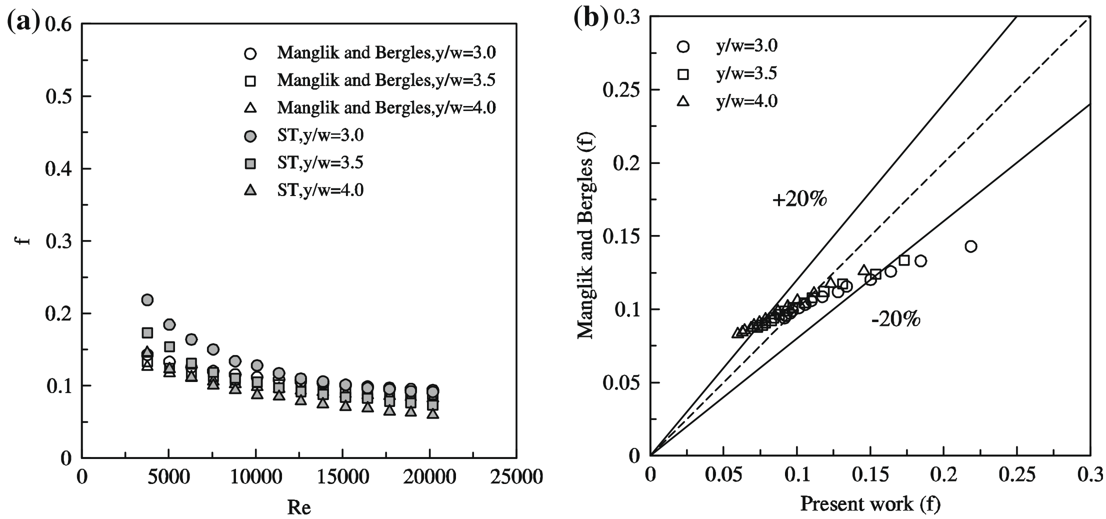

Fig. 5. Confirmatory test of friction factor of single twisted tape: (a) *f* and *Re* and (b) deviation of the present *f* from those by Manglik and Bergles [16].

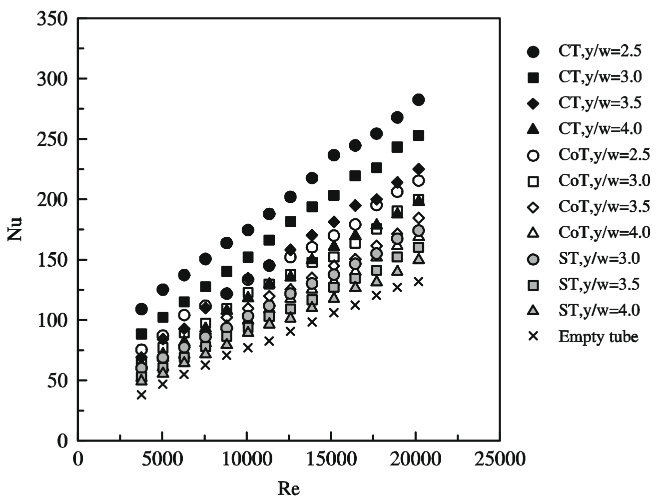

Fig. 6. Variations of Nusselt number with Reynolds number for various twisted tape inserts.

In the present study, the phenomena of the swirling flow in the tube fitted with the *ST*, *CoTs* and *CTs* are demonstrated in Fig. 7a–c using finite volume method [17]. The results are based on the computational conditions as shown in Table 3, for the flow at the constant Reynolds number, *Re* = 10,000. Apparently, twin swirl flows are produced for both *CoTs* and *CTs* while only single swirl flow is generated by the *ST*. The higher number of streams generated by both twin tapes is responsible for a better mixing and thus higher heat transfer rate (*Nu*) as experimental results shown in Fig. 6. For all twisted tapes, each stream is induced along each side of tape with axisymmetric profile in direction led by the tape geometry. With the close look for twin co-twisted tapes (*CoTs: co-swirl flow generators*), recirculation zones appear on the top/bottom of vortex core and the generated swirl flows show just small contact zone in the clearance between two twisted tapes, indicating little interaction between them. Therefore, the mixing in the tube equipped with the *CoTs* is dominantly enhanced by rather independent swirl flows. On the other hand, the swirls generated by twin counter twisted tapes (*CTs: counter-swirl flow generators*) are found to be converged in the clearance between two twisted tapes, this apparently provides higher intensity of vortex strength than that gener-

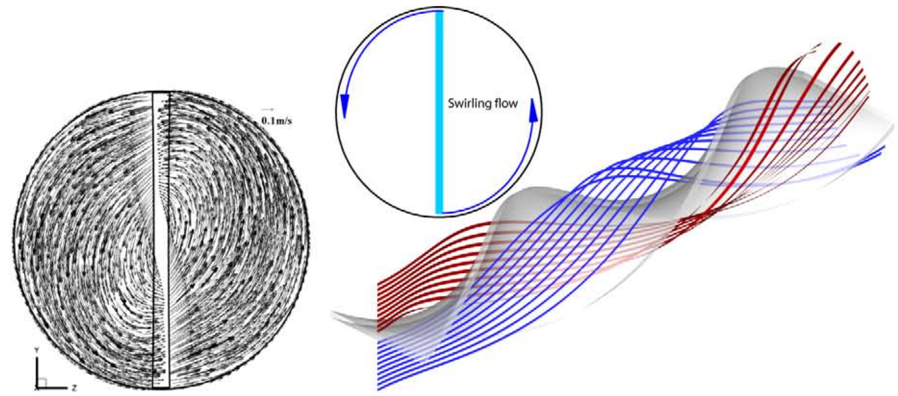

(a) *single twisted tape (ST)*

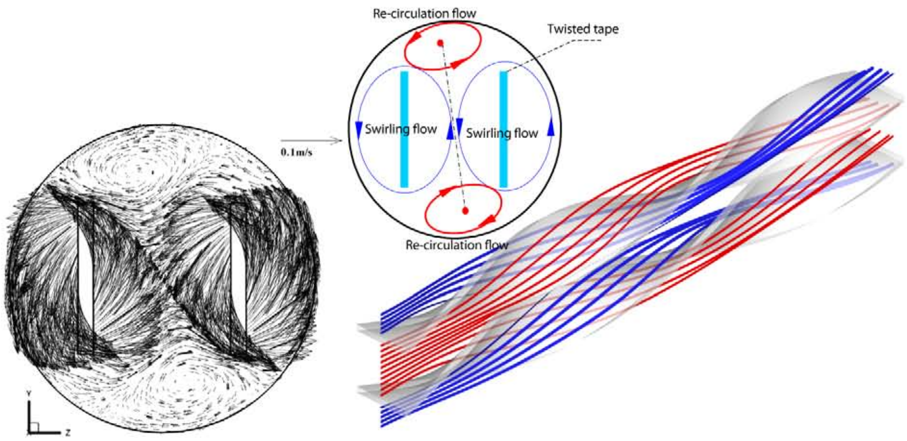

(b) *twin co twisted tapes (CoTs)*

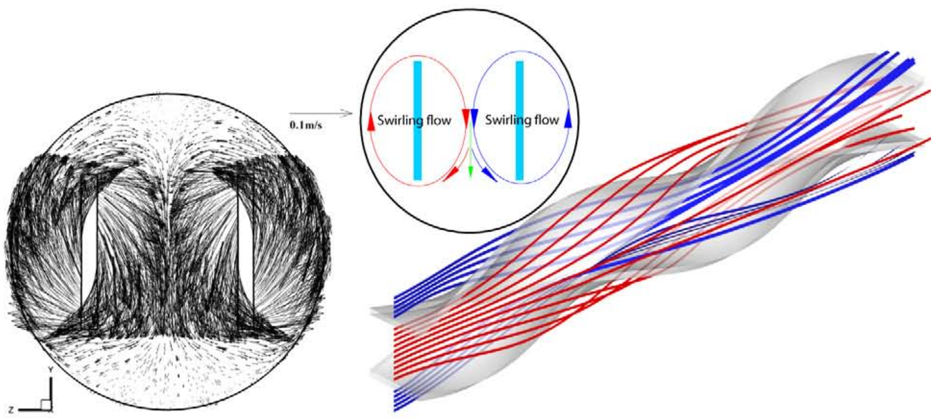

(c) *twin counter twisted tapes (CTs)*

Fig. 7. Path line of flow through a tube fitted with twisted tape: (a) single twisted tape (*ST*), (b) twin co-twisted tapes (*CoTs*) and (c) twin counter twisted tapes (*CTs*).

ated by the *CoTs*. In addition, the recirculation zone is not induced in the tube with the *CTs* as the strong swirl flows impinge to the tube wall. Therefore, it can be addressed herein that the higher interaction between swirl flows (or high vortex strength) induced by the *CTs* leads to superior fluid mixing, resulting in uniform fluid temperature in tubes, and thus more efficient heat transfer in comparison with the *CoTs*. This confirmed by the obtained results in which, the heat transfer rates in the tube fitted with the *CTs* (counter-swirl flow) are noticeably higher than those in the tube fitted with the *CoTs* (co-swirl flow) for all range Reynolds numbers studied (Fig. 6). From the figure, it is also found that the influence of the *CTs* on the heat transfer rate is more intense at higher Reynolds number. Over the range considered, heat transfer rate in the tubes fitted with *CTs* are, respectively, 12.5–44.5% and 17.8–50% higher than those in tubes equipped with the *CoTs* (*co-swirl flows*) and the *ST* (*single swirl flow*).

Fig. 8 presents the friction factor in the corresponding tubes as shown in Fig. 6. Basically, the friction factor decreases with increasing Reynolds number. At the same Reynolds number, the friction factors in the tube fitted with the *CTs* are higher than those in tube fitted with the *CoTs*, tube fitted with the single twisted tape (*ST*) and the empty tube (*non-swirl flow*). This is a consequence of

Table 3
Details of computational conditions.

Twisted tape	*ST*	*CTs*	*CoTs*
(a) Dimensional	3D	3D	3D
(b) Number of grid generation (nodes)	261,495	255,712	254,671
(c) Method	Finite volume	Same as *ST*	Same as *ST*
(d) Turbulence modeling	k–ε model with QUICK	Same as *ST*	Same as *ST*
(e) Flow condition	Isothermal flow	Same as *ST*	Same as *ST*
(f) Fluid	Water	Same as *ST*	Same as *ST*
(g) Inlet temperature	25 °C	Same as *ST*	Same as *ST*
(h) Reynolds number	10,000	Same as *ST*	Same as *ST*
(i) Flow condition	Isothermal flow	Same as *ST*	Same as *ST*

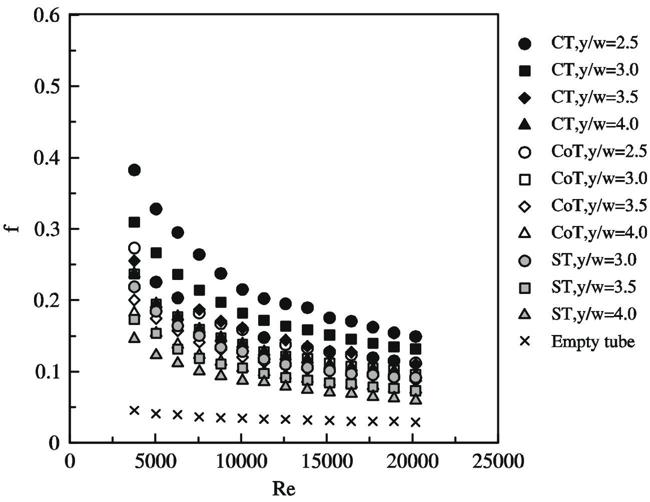

Fig. 8. Variations of friction factor with Reynolds number for various twisted tape inserts.

the repeated acts of strong intensity of vortex in the tube with *CTs*. Over the range studied, the friction factors for tube fitted with *CTs* are higher than those in tube fitted with the *CoTs* around 26.5–45.5%.

5.3. Effect of twist ratios

Effect of twist ratios (y/w = 2.5, 3.0, 3.5 and 4.0) on the heat transfer rate in the tube fitted with *CTs* and *CoTs* is demonstrated in Fig. 6. From the experimental results, it can be observed that heat transfer enhancement increase as twist ratio decreases. In common, the smaller twist ratio generates stronger swirl intensity, leading to more efficient interruption of boundary layer along the flow path. Hence, heat can be transferred efficiently over thin boundary layer. Moreover, the residence time of the flow increases with the increasing swirl flow intensity [7]. This extend the duration of heat transfer between the working fluid and heat source (tube wall). For the entire conditions studied, the *CTs* and *CoTs* with the smallest twist ratio (y/w = 2.5) provide the heat transfer rates around 7.8 to 74.6% and 59.4–187% higher than those for the tube with larger twist ratios and the empty tube, respectively.

As seen in Fig. 8, friction factor tends to increase with decreasing twist ratio. This is in the same trend found for Nusselts number. This can be explained by the fact that the use of a twisted tape with a smaller twist ratio leads to a higher viscous loss near the tube wall regions caused by a stronger swirl flow. Over the range studied, the friction factors for the tube fitted with *CTs* with y/w = 2.5, 3.0, 3.5 and 4.0, are, respectively, 6.37, 5.33, 4.57 and 3.95 times of those in the empty tube.

In the present investigation, the tests are made in a uniform heat flux tube with water as working fluid and correlations are applicable to turbulent region of Reynolds number (*Re*) between 3700 and 21,000. The empirical correlations from the experimental results of the empty tube fitted with the *ST*, *CoTs* and *CTs* can be writing in term of twist ratio (y/w), Reynolds number (*Re*) and Prandtl number (*Pr*) as follows:

The tube fitted with the ST:

$$Nu = 0.224Re^{0.66}Pr^{0.4}(y/w)^{-0.6} \tag{11}$$

$$f = 65.4Re^{-0.52}(y/w)^{-1.31} \tag{12}$$

The tube fitted with the CTs (counter-swirl flow generators):

$$Nu = 0.473Re^{0.66}Pr^{0.4}(y/w)^{-0.9} \tag{13}$$

$$f = 72.29Re^{-0.53}(y/w)^{-1.01} \tag{14}$$

The tube fitted with the CoTs (co-swirl flow generators):

$$Nu = 0.264Re^{0.66}Pr^{0.4}(y/w)^{-0.61} \tag{15}$$

$$f = 41.7Re^{-0.52}(y/w)^{-0.84} \tag{16}$$

Comparisons between the present data with those calculated by the present correlations are for Nusselt number and friction factor portrayed in Figs. 9 and 10. Evidently, the majority of the heat transfer data falls within ±10% for the present correlations of Eqs. (11), (13) and (15). Eqs. (12), (14) and (16) provide the correlative

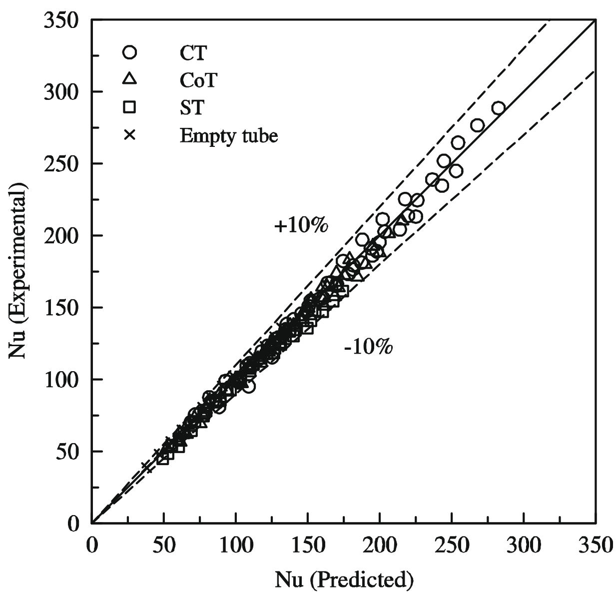

Fig. 9. Validation of empirical correlations for Nusselt number.

results of the friction factor with maximum discrepancies of ±6% with the experimental measurements.

6. Enhancement index

In order to assess the heat transfer enhancement index or thermal enhancement index of the tube fitted with the *CTs* and the *CoTs*, a equal pumping power comparison is performed [18–20]. At the constant pumping power, the relationship between volumetric flow rate and the pressure loss between the empty tube and the tube fitted with the *CTs*/*CoTs* is written as:

$$(\dot{V}\Delta P)_e = (\dot{V}\Delta P)_s \tag{17}$$

and the relationship between friction and Reynolds number is expressed as:

$$(fRe^3)_e = (fRe^3)_s \tag{18}$$

The thermal enhancement index is defined as:

$$\eta = \left.\frac{h_s}{h_e}\right|_{pp} \tag{19}$$

where h_s is the heat transfer coefficient for the empty tube with the *CTs* or *CoTs* insert while h_e is the heat transfer coefficient for the empty tube, at identical pumping power.

Performance evaluation is determined to asses the benefits of using the *CTs* and the *CoTs* in term of enhancement index at the same pumping power. Applying Eqs. (10), (12/14/16) and (18), the Reynolds number for the empty tube (Re_e) can be expressed as the function of the Reynolds number of the tube fitted with twisted tape (Re_s):

For the tube fitted with the ST (Re_s):

$$Re_e = 6.57Re_s^{0.9}(y/w)^{-0.48} \tag{20}$$

For the tube fitted with the CTs (Re_s):

$$Re_e = 6.81Re_s^{0.9}(y/w)^{-0.37} \tag{21}$$

For the tube fitted with the CoTs (Re_s):

$$Re_e = 5.57Re_s^{0.9}(y/w)^{-0.31} \tag{22}$$

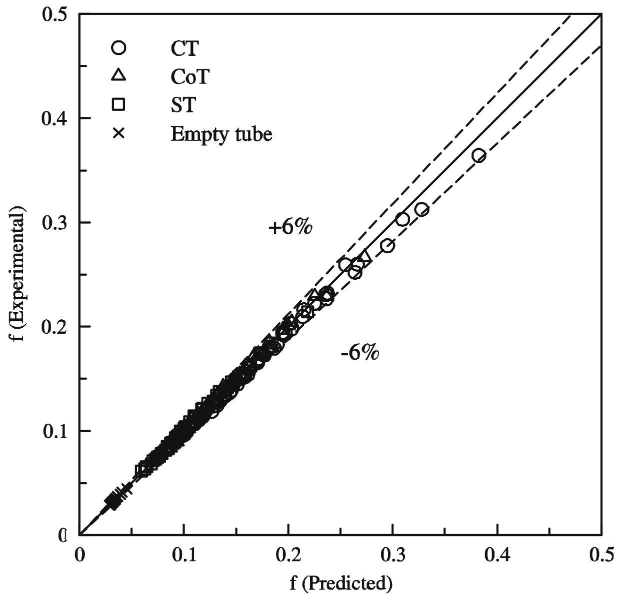

Fig. 10. Validation of empirical correlations for friction factor.

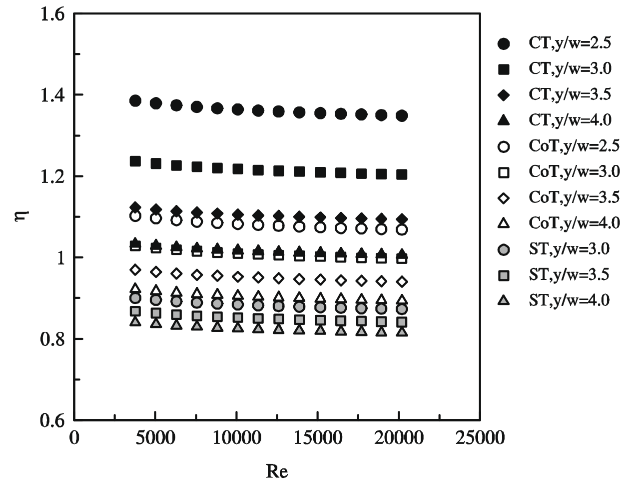

Fig. 11. Variations of thermal enhancement index with Reynolds number for various twisted tape inserts.

Using Eqs. (9), (11), (19) and (20), the thermal enhancement index for tube fitted with *ST* can be expressed as:

$$\eta = 1.365Re_s^{-0.0185}(y/w)^{-0.24} \tag{23}$$

Similarly, the thermal enhancement index for the tube fitted with the *CTs* or *CoTs* can be obtained by the combination of Eqs. (9), (13/15), (19) and (21/22), as follows:

For the tube fitted with the CTs:

$$\eta = 2.8Re_s^{-0.016}(y/w)^{-0.624} \tag{24}$$

For the tube fitted with the CoTs:

$$\eta = 1.82Re_s^{-0.0186}(y/w)^{-0.38} \tag{25}$$

Fig. 11 shows the effect of various single/twin twisted tapes at different twist ratios (y/w) on the thermal enhancement index in Reynolds number range of 3700–21,000. The comparative data reveal that the thermal enhancement index increases with decreasing Reynolds number. In additions, thermal enhancement indices are varied between 1.01 and 1.39 for the *CTs*, 0.89 and 1.1 for the *CoTs*, and 0.81 and 0.9 for the *ST*, depending upon the Reynolds number and the twist ratio (y/w). For the *CTs*, the mean enhancement index for the smallest twist ratio (y/w = 2.5) is, respectively, 12%, 23.4% and 34% higher than those for y/w = 3.0, 3.5 and 4.0. The above data suggest that the highest enhancement index can be obtained at the low twist ratio (y/w), and relatively low Reynolds number. It is noteworthy that the enhancement indices in the tube fitted with the *CTs* (*counter-swirl tapes*) are around 12–25.7% higher than those in the tube fitted with the *CoTs* (*co-swirl tapes*).

7. Conclusions

The present paper shows the feasibility of convection heat transfer enhancement by inserting the *CTs* (*counter-swirl flow generators*) and the *CoTs* (*co-swirl flow generators*) for turbulent flow with a uniform heat flux. Heat transfer coefficient and friction factor are determined experimentally for the tube fitted with the *CTs*, *CoTs* and *ST* using water as working fluid with Reynolds number ranging from 3700 to 21,000. Based on the obtained results, key findings of this investigation can be summarized as follows:

(I) For general observation, it is found that heat transfer, friction factor, and thermal enhancement index increase as the twist ratio (y/w) decreases. In addition, the Nusselt number increases with increasing Reynolds number while the opposite trends are found for the friction factor and the thermal enhancement index.

(II) The *CTs* (*counter-swirl tapes*) can enhance heat transfer more efficiently than the *CoTs* (*co-swirl tapes*). The quantitative results show that, heat transfer rates for the *CTs* are around 12.5–44.5% higher than those for the *CoTs* and around 17.8–50% higher than those for the *ST*. The maximum thermal enhancement indices (η) obtained at the constant pumping power by using the *CTs* with y/w = 2.5, 3.0, 3.5 and 4.0, are 1.39, 1.24, 1.12 and 1.03, respectively, while those obtained by using the *CoTs* with the same range of y/w are 1.1, 1.03, 0.97 and 0.92. The achieved results indicate that the modified swirl flow (*counter-swirl flow*) generated by the *CTs* is a promising approach for heat transfer enhancement.

(III) The empirical correlations developed in the present work, provide the correlative results of the Nusselt number and friction factor. The maximum discrepancies between the correlative results and experimental results for Nusselt number and friction factor are found to be ±10% and ±6%, respectively.

Acknowledgement

The first author would like to gratefully acknowledge the Thailand Research Fund (*TRF*) for the financial support of this research.

References

[1] J.M. Whitham, The effects of retarders in fire tubes of steam boilers, Street Railway Journal 12 (1896) 374.
[2] G.C. Kidd Jr., Heat transfer and pressure drop for nitrogen flowing in tubes containing twisted tapes, AIChE Journal 15 (1969) 581–585.
[3] O.H. Klepper, Heat transfer performance of short twisted tapes, AIChE Journal 35 (1972) 1–24.
[4] S.K. Saha, U.N. Gaitonde, A.W. Date, Heat transfer and pressure drop characteristics of laminar flow in a circular tube fitted with regularly spaced twisted-tape elements, Experimental Thermal Fluid Science 2 (1989) 310–322.
[5] A.W. Date, U.N. Gaitonde, Development of correlations for predicting characteristics of laminar flow in a tube fitted with regularly spaced twisted-tape elements, Experimental Thermal Fluid Science 3 (1990) 373–382.
[6] J.K. Dasmahapatra, M. Raja Rao, Laminar flow heat transfer to generalized power law fluids inside circular tubes fitted with regularly spaced twisted tape elements for uniform wall temperature condition, Heat Transfer Division HTD, ASME 174 (1991) 51–58.
[7] S. Eiamsa-ard, C. Thianpong, P. Promvonge, Experimental investigation of heat transfer and flow friction in a circular tube fitted with regularly spaced twisted tape elements, International Communications in Heat and Mass Transfer 33 (2006) 1225–1233.
[8] S.W. Chang, K.W. Yu, M.H. Lu, Heat transfer in tubes fitted with single, twin and triple twisted tapes, Experimental Heat Transfer 18 (2005) 279–294.
[9] S.W. Chang, Y.J. Jan, J.S. Liou, Turbulent heat transfer and pressure drop in tube fitted with serrated twisted-tape, International Journal Thermal Sciences 46 (2007) 506–518.
[10] S.W. Chang, T.L. Yang, J.S. Liou, Heat transfer and pressure drop in tube with broken twisted tape insert, Experimental Thermal and Fluid Science 32 (2008) 489–501.
[11] M. Rahimi, S.R. Shabanian, A.A. Alsairafi, Experimental, CFD studies on heat transfer and friction factor characteristics of a tube equipped with modified twisted tape inserts, Chemical Engineering and Processing 48 (3) (2009) 762–770.
[12] P. Bharadwaj, A.D. Khondge, A.W. Date, Heat transfer and pressure drop in a spirally grooved tube with twisted tape insert, International Journal of Heat and Mass Transfer 52 (7–8) (2009) 1938–1944.
[13] S. Jaisankar, T.K. Radhakrishnan, K.N. Sheeba, Experimental studies on heat transfer and friction factor characteristics of thermosyphon solar water heater system fitted with spacer at the trailing edge of twisted tapes, Applied Thermal Engineering 29 (5–6) (2009) 1224–1231.
[14] A. Dewan, P. Mahanta, K. Sumithra Raju, P. Suresh Kumar, Review of passive heat transfer augmentation techniques, Journal of Power and Energy 218 (2004) 509–525.
[15] F.P. Incropera, P.D. Witt, T.L. Bergman, A.S. Lavine, Fundamentals of Heat and Mass Transfer, John-Wiley & Sons, 2006.
[16] R.M. Manglik, A.E. Bergles, Heat transfer and pressure drop correlations for twisted-tape inserts in isothermal tubes: part II – transition and turbulent flows, Transaction of ASME, Journal Heat Transfer 115 (1993) 890–896.
[17] S. Eiamsa-ard, K. Wongcharee, S. Sripattanapipat, 3-D Numerical simulation of swirling flow and convective heat transfer in a circular tube induced by means of loose-fit twisted tapes, International Communications in Heat and Mass Transfer, in press, Uncorrected proof, Available online 19 July 2009.
[18] R.L. Webb, N.H. Kim, Principles of Enhanced Heat Transfer, second ed., Taylor & Francis, New York, 2005.
[19] K. Yakut, B. Sahin, S. Canbazoglu, Performance and flow-induced vibration characteristics for conical-ring turbulators, Applied Energy 79 (2004) 65–76.
[20] K. Bilen, U. Akyol, S. Yapici, Heat transfer and friction correlations and thermal performance analysis for a finned surface, Energy Conversion and Management 42 (2001) 1071–1083.


Volume 36 Number 9
November 2009
ISSN 0735-1933
ELSEVIER
International Communications in
HEAT and MASS TRANSFER
Editor-in-Chief
W.J. MINKOWYCZ
Editors
A.R. BALAKRISHNAN, P. CHENG, R. GREIF, C.P. GRIGOROPOULOS, E. HAHNE,
A.I. LEONTIEV, O.G. MARTYNENKO, J.W. ROSE, J. TAINE, H. YOSHIDA
Available online at
ScienceDirect
www.sciencedirect.com

International Communications in Heat and Mass Transfer 36 (2009) 947–955

Contents lists available at ScienceDirect

International Communications in Heat and Mass Transfer

journal homepage: www.elsevier.com/locate/ichmt

3-D Numerical simulation of swirling flow and convective heat transfer in a circular tube induced by means of loose-fit twisted tapes ☆

S. Eiamsa-ard [a,*], K. Wongcharee [b], S. Sripattanapipat [a]

[a] Department of Mechanical Engineering, Faculty of Engineering, Mahanakorn University of Technology, Bangkok 10530, Thailand
[b] Department of Chemical Engineering, Faculty of Engineering, Mahanakorn University of Technology, Bangkok 10530, Thailand

ARTICLE INFO

Available online 19 July 2009

Keywords:
Loose-fit twisted tape
Heat transfer enhancement
Heat exchanger
Swirl flow

ABSTRACT

The article presents the application of a mathematical model for simulation of the swirling flow in a tube induced by loose-fit twisted tape insertion. Effects of the clearance ratio defined as ratio of clearance between the edge of tape and tube wall to tube diameter ($CR = c/D = 0.0$ (tight-fit), 0.1, 0.2 and 0.3) on heat transfer enhancement (Nu), friction factor (f) and thermal performance factor (η) are numerically investigated for twisted tapes at two different twist ratios ($y/w = 2.5$ and 5.0). The simulation is conducted in order to gain an understanding of physical behavior of the thermal and fluid flow in the tube fitted with loose-fit twisted tape under constant wall temperature conditions in the turbulent flow regime for the Reynolds number ranging from 3000 to 10,000. The Navier–Stokes equation in common with a energy equation is solved using the SIMPLE technique with the standard k–ε turbulence model, the Renormalized Group (RNG) k–ε turbulence model, the standard k–ω turbulence model, and Shear Stress Transport (SST) k–ω turbulence model. The numerical results show that the predictions of heat transfer (Nu) and friction factor (f) based on the SST k–ω turbulence models are in better agreement with Manglik and Bergles [R.M. Manglik, A.E. Bergles, Heat transfer and pressure drop correlations for twisted-tape inserts in isothermal tubes, part II: Transition and turbulent flows, Transaction ASME, Journal of Heat Transfer, 115 (1993) 890–896.] than other turbulence models. The mean flow patterns in a tube with loose-fit twisted tapes in terms of contour plots of velocity, pathline, pressure, temperature and turbulent kinetics energy (TKE) are presented and compared with those in a tube fitted with tight-fit twisted tapes. It is visible that the twisted tape inserts for $y/w = 2.5$ with $CR = 0.0$ (tight-fit), 0.1, 0.2 and 0.3 can enhance heat transfer rates up to 73.6%, 46.6%, 17.5% and 20%, respectively and increase friction factors up to 330%, 262%, 189%, and 160%, respectively, in comparison with those of the plain tube. The tube with loose-fit twisted tape inserts with $CR = 0.1$, 0.2 and 0.3 provide heat transfer enhancement around 15.6%, 33.3% and 31.6% lower than those with $CR = 0.0$ (the tight-fit twisted tape). The heat transfer augmentation is expected to involve the swirl flow formation between the tape and a tube wall. In addition, the simulation for thermal performance factor (η) of a tube with the loose-fit twisted tape and the tight-fit twisted tape under the same pumping power is also conducted, for comparison.

1. Introduction

Twisted tape swirl generators are utilized as passive heat transfer enhancement devices which work without any external power source. Twisted tapes have been applied in several systems such as shell and tube heat exchanger, solar water heater, boiler and chemical engineering process, etc. The tapes have gained rising attention, due to their advantages of steady performance, simple configuration and ease of installation. In addition, twisted tapes have also shown to increase significantly the heat transfer coefficient with a relatively small pressure loss penalty. The tapes interrupt the hydrodynamic/thermal boundary layer and form a swirl flow along the flow through and create a series of thin boundary layers which have lower thermal resistance than thick boundary layer, appearing in the plain tube. The twisted tapes also increase the residence time and normal gradients of the velocity and turbulence intensity near the tube wall, contributing to heat transfer enhancement. The investigations on heat transfer and flow friction in tubes fitted with twisted tapes with various tape geometries have been conducted by many researchers for both experimental and numerical works [1–13].

Computational technology advancement during the past decades has extended the ways of finding solutions of the complicated mathematical equations by numerical analysis, especially Computational Fluid Dynamics (CFD). Some reports of numerical analysis for

☆ Communicated by W.J. Minkowycz.

* Corresponding author.
E-mail address: smith@mut.ac.th (S. Eiamsa-ard).

0735-1933/$ – see front matter © 2009 Elsevier Ltd. All rights reserved.
doi:10.1016/j.icheatmasstransfer.2009.06.014

Nomenclature

CR	clearance ratio $= c/D$
C_μ	turbulence model constant
D	inner tube diameter, m
E	total energy, J
f	friction factor
h	enthalpy, J or convective heat transfer coefficient, W m^{-2} K^{-1}
k	thermal conductivity, W m^{-1} K^{-1}
k_{eff}	effective thermal conductivity, W m^{-1} K^{-1}
L	test section length, m
Nu	Nusselt number
p	static pressure, Pa
Δp	pressure drop, Pa
Re	Reynolds number
u	mean velocity, m s^{-1}
u_i'	fluctuation velocity components, m s^{-1}
w	tape width, m
y	twist length, m

Greek symbols

μ	kinematic viscosity, kg s^{-1} m^{-1}
μ_t	eddy viscosity, kg s^{-1} m^{-1}
η	thermal performance factor, $((\mathrm{Nu}/\mathrm{Nu}_0)/(f/f_0)^{1/3})$
ε	turbulent dissipation rate, m^2 s^{-3}
ρ	density, kg m^{-3}
δ_{ij}	Kronecker delta

Subscript

ave	average
0	plain tube

the tubes fitted with twisted tapes, are declared as follows. Date and Singham [1] reported a numerical investigation of heat transfer augmentation in viscous liquid laminar flows in tubes fitted with twisted tape under uniform heat flux boundary condition. In their work, the influences of the twist and fin were examined with assumption of zero tape thickness. Date [2] also proposed a numerical analysis of flows in the tube with twisted tape inserts for fully developed and uniform flows. Du Plessis [3] investigated numerically the heat transfer and fluid flow characteristics in a tube with twisted tape insert under isothermal boundary layer condition, for laminar flow. Later on, Du Plessis and D.G. Kroger [4] predicted the friction factor in a tube fitted with twisted tape for fully developed laminar flow. After their previous works, Date and Saha [5] used the Navier–Stokes and energy equations in their three-dimensional parabolic form to predict the heat transfer and fluid flow behaviors in a uniform heat flux tube fitted with regularly spaced twisted tape elements. Date [6] also presented numerical prediction of laminar flow and heat transfer in a tube fitted with twisted tape swirl generator. In their work, the influences of property variations and buoyancy on system calculations are also determined. Ray and Date [7] solved a non-staggered non-orthogonal grid using the curvilinear version of the "Complete Pressure Correction" algorithm to predict the laminar flow and heat transfer characteristics of square duct fitted with twisted tape. Again, Ray and Date [8] extended their work to predict the periodic turbulent flow and heat transfer rate in a square duct with twisted tape insert under axially and peripherally constant wall heat flux conditions. Sarma et al. [9] modified the eddy diffusivity expression of van Driest to predict the convective heat transfer coefficient, friction factor and thermal-hydraulic performance in a tube fitted with twisted tapes with a different pitch to diameter ratios. Their finding indicated that the proposed analysis is in reasonable agreement with the well known correlations. Zimparov [10,11] conducted a simple simulation to predict the friction factor and heat transfer coefficient for turbulent flow in spirally corrugated tubes combined with twisted tape inserts. Kazuhisa et al. [12] numerically studied the effect of secondary flow generated on the temperature field mixing and heat transfer enhancement mechanism as well as the effect of gravity on the transition process of secondary flow, flow pattern and the local Nusselt number under a uniform heat flux condition. Rahimi et al. [13] used the RNG k–ε turbulence model to predict the heat transfer enhancement, friction factor and performance ratio in a tube with various twisted tape inserts (perforated, notched and jagged tapes). The phenomenon of flow (tangential velocity and turbulent intensity) through twisted tape is also described.

Above-mentioned literature review demonstrates the extensively numerical works for heat transfer in the tubes equipped with twisted tapes. However, so far, the numerical study on the phenomena of heat and fluid flow through a round tube with loose-fit twisted tape swirl generators has not been reported. Therefore, the aim of the current study is to report details of the turbulence modeling to help in understanding of the behaviors of the incompressible swirl flows for tube fitted with the loose-fit twisted tapes in comparison with those for a tube equipped with tight-fit twisted tapes. In this work, the standard k–ε turbulence model, the Renormalized Group (RNG) k–ε turbulence model, the standard k–ω turbulence model, and the Shear Stress Transport (SST) k–ω turbulence model, are performed to study the phenomena of flow field (velocity vector and streamline), temperature field, pressure field and turbulent intensity (TKE) in a tube with twisted tape inserts. Comparisons of the Nusselt number and friction factor of twisted tape with previous correlation [14] are made to evaluate the turbulence models used. The mathematical models including the turbulence models, numerical solution and other computational details are described. Effects of the clearance ratio (CR = 0.0 (tight-fit), 0.1, 0.2 and 0.3) and twist ratio (y/w = 2.5 and 5.0) on heat transfer rate (Nu), friction factor (f) and thermal performance factor (η) are examined under constant wall temperature using water as the testing fluid. Furthermore, the influence of grid generation on prediction results is also reported.

2. Mathematical foundation

The mathematical modeling involves the prediction of flow and heat transfer behaviors. The available finite difference procedures for swirling flows and boundary layer are employed to solve the governing partial equations. Some simplifying assumptions are required for applying of the conventional flow equations and energy equations to model the heat transfer process in tube with twisted tape. The major assumptions are; (1) the flow through the twisted tape is turbulent and incompressible, (2) the flow is in steady state, (3) natural convection and thermal radiation are neglected and (4) the thermo-physical properties of the fluid are temperature independent.

2.1. Governing equations

Based on above the approximations, the governing differential equations used to describe the fluid flow and heat transfer in round tubes with twisted tape inserts are established. The continuity, momentum and energy equations for the three-dimensional models are employed. For steady state, constant density flows, the timeaveraged incompressible Navier–Stokes equations in the Cartesian tensor notation can be written in the following form:

Continuity equation:

$$\frac{\partial}{\partial x_i}(\rho u_i) = 0. \tag{1}$$

Momentum equation:

$$\frac{\partial\left(\rho u_i u_j\right)}{\partial x_j} = -\frac{\partial p}{\partial x_i} + \frac{\partial}{\partial x_j}\left[\mu\left(\frac{\partial u_i}{\partial x_j} + \frac{\partial u_j}{\partial x_i} - \frac{2}{3}\delta_{ij}\frac{\partial u_k}{\partial x_k}\right)\right] + \frac{\partial}{\partial x_j}\left(-\rho\overline{u_i' u_j'}\right). \tag{2}$$

Energy equation:

$$\frac{\partial}{\partial x_i}[u_i(\rho E + p)] = \frac{\partial}{\partial x_j}\left(k_{\mathrm{eff}}\frac{\partial T}{\partial x_j}\right). \tag{3}$$

$$E = h - \frac{p}{\rho} + \frac{u^2}{2}. \tag{4}$$

The Reynolds-averaged approach to turbulence modeling requires that the Reynolds stresses, $-\rho\overline{u_i' u_j'}$ in Eq. (2) be appropriately modeled. A common method employs the Boussinesq hypothesis to relate the Reynolds stresses to the mean velocity gradients:

$$-\rho\overline{u_i' u_j'} = \mu_t\left(\frac{\partial u_i}{\partial x_j} + \frac{\partial u_j}{\partial x_i}\right) - \frac{2}{3}\left(\rho k + \mu_t\frac{\partial u_k}{\partial x_k}\right)\delta_{ij}. \tag{5}$$

The turbulent viscosity term μ_t is to be computed from an appropriate turbulence model. The expression for the turbulent viscosity is given as

$$\mu_t = \rho C_\mu \frac{k^2}{\varepsilon}. \tag{6}$$

In contrast to the molecular viscosity, the eddy viscosity depends strongly on flow properties. Therefore, selecting a turbulence model, accommodated the flow behavior of each application, is very important. To attain the accurate aerodynamic prediction in tube with twisted tape insert, the predictive ability of four different turbulence models, including, the standard k–ε turbulence model, the Renormalized Group (RNG) k–ε turbulence model, the standard k–ω turbulence model, and the Shear Stress Transport (SST) k–ω turbulence model, is examined.

2.2. Solution procedure

In the present numerical solution, the time-independent incompressible Navier–Stokes equations and the various turbulence models are discretized using the finite volume technique. QUICK (Quadratic upstream interpolation for convective kinetics differencing scheme) and central differencing flow numerical schemes are applied for convective and diffusive terms, respectively. To evaluate the pressure field, the pressure–velocity coupling algorithm SIMPLE (Semi Implicit Method for Pressure-Linked Equations) is selected. Impermeable boundary condition is implemented over the tube wall. The turbulence intensity is kept at 10% at the inlet, unless other-wise stated. The solution convergence is met when the difference between normalized residual of the algebraic equation and the prescribed value is less than 10^{-6}.

Three parameters of interest for the present work are: (1) friction factor, (2) Nusselt number and (3) thermal performance factor which respectively used for characterization of friction loss, heat transfer

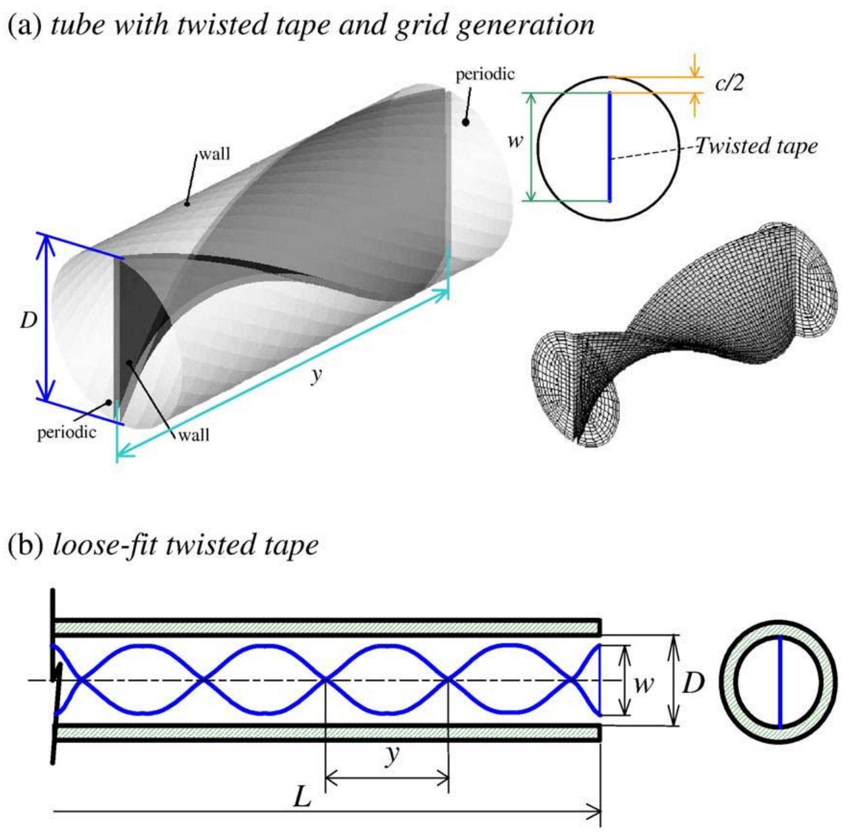

Fig. 1. Geometry of round tubes with twisted tape inserts: (a) tube with twisted tape and grid generation and (b) loose-fit twisted tape.

rate, and effectiveness of heat transfer enhancement in the tube with twisted tape insert for a given geometry and flow conditions. The friction factor, f is computed from pressure drop, Δp across the length of the tube, L using following equation:

$$f = \frac{\Delta p / L}{\frac{1}{2}\rho u^2 D}. \tag{7}$$

The Nusselt number is defined as:

$$\mathrm{Nu} = \frac{hD}{k}. \tag{8}$$

The average Nusselt number can be obtained by

$$\mathrm{Nu}_{\mathrm{ave}} = \int \mathrm{Nu}(x)\partial x / L. \tag{9}$$

Thermal performance factor is given by

$$\eta = \frac{(\mathrm{Nu}/\mathrm{Nu}_0)}{(f/f_0)^{1/3}} \tag{10}$$

where Nu_0, Nu, f_0 and f are the Nusselt numbers and friction factors for the plain tube and the tube with twisted tape swirl generator, respectively.

3. Flow configurations

The computational domain for the flow in tube fitted with twisted tape is resolved by regular Cartesian elements, as shown in Fig. 1(a–b). The pattern shown is limited for only 180° twist length due to a periodic flow. The numerical analysis is made for twisted tapes at two different twist ratios, $y/w=2.5$ and 5.0 and four different clearance ratios, CR = 0.0 (tight-fit), 0.1 (loose-fit of 10%), 0.2 (loose-fit of 20%) and 0.3 (loose-fit of 30%). The clearance ratio is defined herein as ratio of clearance between the edge of tape and tube wall to tube diameter (c/D). Grid independent solution is obtained by comparing the solution for different grid levels. The total numbers of elements used are approximately 5472, 8008, 12,200 and 22,968 for $y/w=2.5$ and 35,420, 45,936, 49,750 and 118,162 for $y/w=5.0$. The higher numbers of elements employed for the tape with $y/w=5.0$, are due to the longer twist length in comparison with the tape with $y/w=2.5$. The Reynolds numbers used for the computation are referred to the inlet values which are set at 3000, 4000, 6000, 8000 and 10,000. The inner tube wall and inlet temperatures are kept constant at 310 K and 300 K, respectively while the outer tube wall is maintained under adiabatic condition. For verification, the present results are compared with the experimental results obtained by Manglik and Bergles [14] with similar operation conditions.

4. Numerical results

4.1. Grid independent

In order to assess the grid independent of the numerical solutions, the different total numbers of elements are used as mentioned in Section 3. For $y/w=2.5$, the use of grid systems of 12,200 and 22,968 gives comparable results. The similar situation is also found for the use of grid systems of 49,750 and 118,162 for $y/w=5.0$. Considering both convergent time and solution precision, the grids with 12,200 and 49,750 elements are adopted for the computational model of twisted tapes with $y/w=2.5$ and $y/w=5.0$, respectively.

4.2. Verification of twisted tape

The characteristics of swirling turbulent flows in a round tube with tight-fit twisted tape insert (CR = 0.0) by means of mathematical equations in association with the standard k–ε turbulence model, the Renormalized Group (RNG) k–ε turbulence model, the standard k–ω turbulence model, and Shear Stress Transport (SST) k–ω turbulence model are shown in the Fig. 2(a–b). The predicted results of Nusselt number and friction factor are compared with the experimental results obtained by Manglik and Bergles [14]. It is clearly seen that the predicted Nusselt numbers obtained from the use of the standard k–ω and SST k–ω turbulence models with QUICK scheme are in better agreement with the previous results, compared to those from other models. The computations of the flow also showed that both models show a significant improvement over other models in capturing friction factor behavior. The SST k–ω turbulence models are valid within ±12.2% error limit with measurements for Nusselt number and ±6.4% for friction factor.

4.3. Flow structure

4.3.1. Velocity vector

Vector plots of velocity predicted for twisted tapes with different clearance ratios (CR = 0.0, 0.1, 0.2 and 0.3) and twist ratios ($y/w=2.5$ and 5.0), by SST k–ω model using the QUICK scheme are depicted in Figs. 3(a–d) and 4(a–d). As seen, swirl flow in mainly forward direction is generated around the tapes. However, segment of swirl

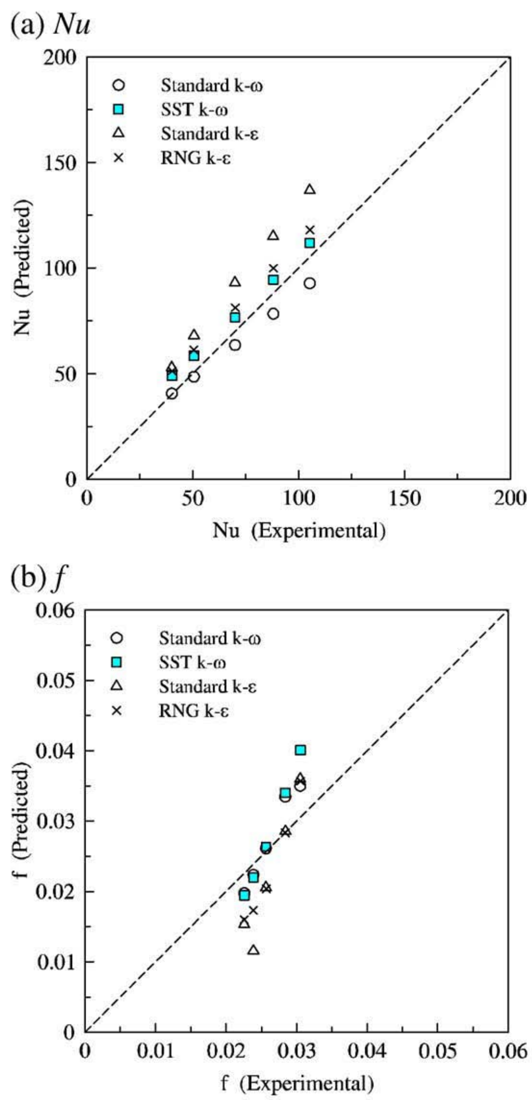

Fig. 2. Comparison of the predicted results with those obtained by Manglik and Bergles [14]: (a) Nu and (b) f.

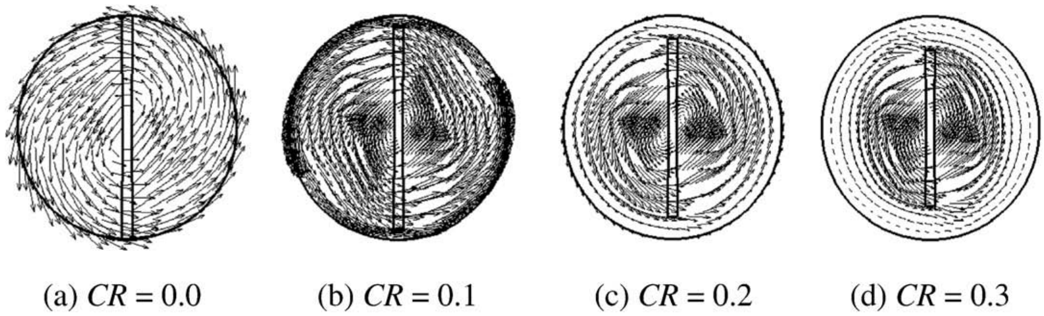

Fig. 3. Vector plots of velocity at different clearance ratios (CR) for $y/w = 2.5$: (a) CR = 0.0, (b) CR = 0.1, (c) CR = 0.2, and (d) CR = 0.3.

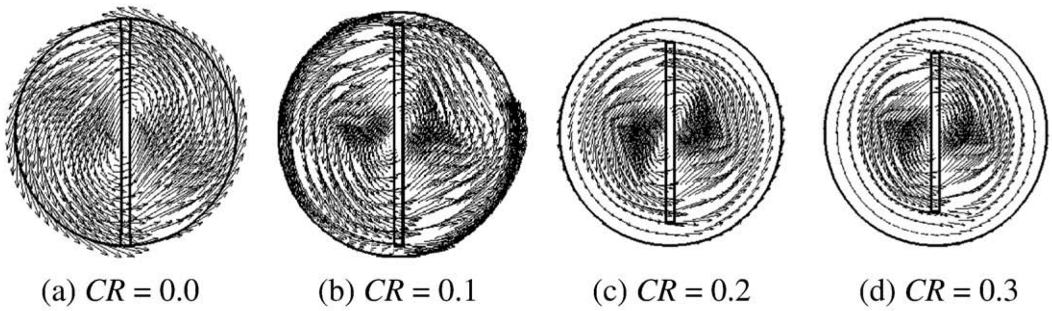

Fig. 4. Vector plots of velocity at different clearance ratios (CR) for $y/w = 5.0$: (a) CR = 0.0, (b) CR = 0.1, (c) CR = 0.2, and (d) CR = 0.3.

flow in the reversed direction is found for only CR = 0.1 at both twist ratios. The vector plots demonstrate that the reversed flow appears in the free spacing area between the tube wall and the edge of the tape.

4.3.2. Streamline

Contour plots of streamline through the tube with twisted tape inserts are respectively displayed in Figs. 5(a–b) and 6(a–b). It is clearly seen that the tape with CR = 0.0 (tight-fit tape) induces only swirling flow while the loose-fit tape CR = 0.1–0.3 generates two types of flows which are (1) a swirling flow and (2) an axial or straight flow near the tube wall. It is noteworthy that the loose tape with smaller clearance ratio (CR = 0.1) gives higher velocity of the fluid flow through the free spacing compared to those with larger clearance ratios (CR = 0.2 and 0.3), due to a smaller free spacing area between the tape and tube wall.

4.3.3. Static pressure

Contour plots of static pressure predicted for twisted tapes with different clearance ratios (CR = 0.0, 0.1, 0.2 and 0.3) and twist ratios ($y/w = 2.5$ and 5.0) are shown in Figs. 7(a–d) and 8(a–d). Obviously, the high static pressure is appeared in the contact zone of the flowing fluid and tube wall affected by tangential contact between them, which is associated by swirl flow. This effect is the most intense for tight-fit twisted tape (CR = 0.0) with the lower twist ratio ($y/w = 2.5$). The increases of clearance ratio as well as twist ratio are found to weaken the effect which is attributed to the reduction of swirl flow intensity.

4.3.4. Temperature field

Figs. 9(a–d) and 10(a–d) show the contour plots of temperature fields for tight-fit twisted tape (CR = 0.0) and loose-fit twisted tapes (CR = 0.1, 0.2 and 0.3). For both twist ratios, the loose-fit twisted tapes with clearance ratio, CR = 0.1 provide better temperature distribution than the twisted tapes with larger clearance ratios, CR = 0.2 and 0.3. This is attributed to more efficient mixing inside the tube fitted with the twisted tape with CR = 0.1 which is influenced by a stronger swirl flow and also reversed flow appearing only with the use of the tape at the mentioned clearance ratio. The low intensity of swirl flow as well as an

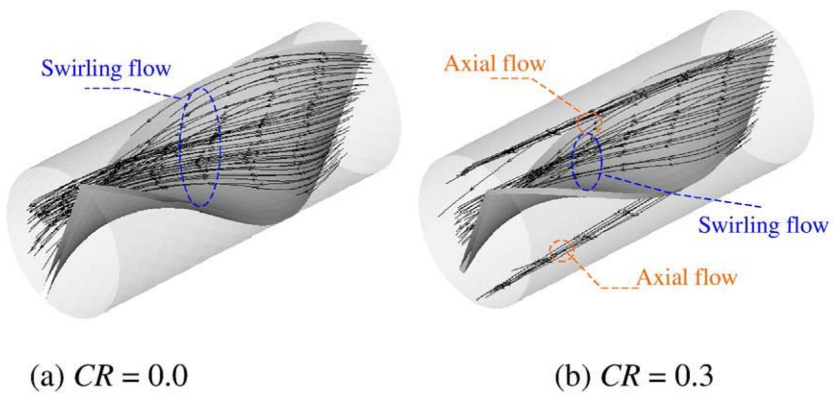

Fig. 5. Contour plots of streamline at different clearance ratios (CR) for $y/w = 2.5$: (a) CR = 0.0 and (b) CR = 0.3.

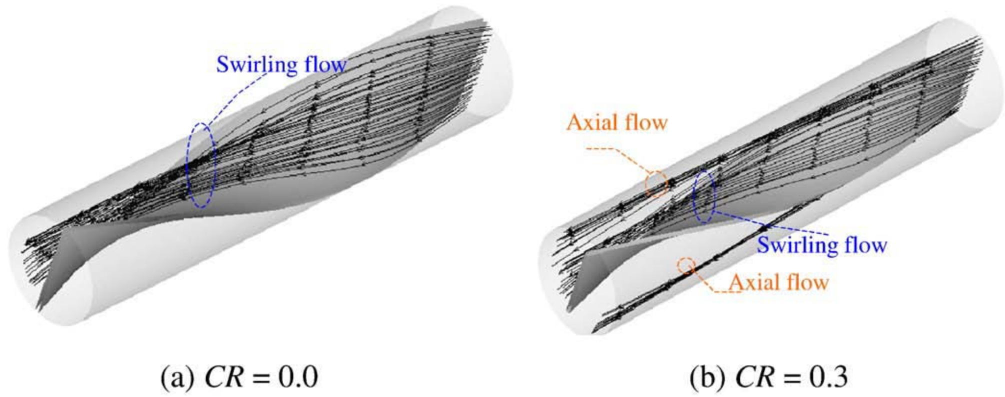

Fig. 6. Contour plots of streamline at different clearance ratios (CR) for $y/w = 5.0$: (a) CR = 0.0 and (b) CR = 0.3.

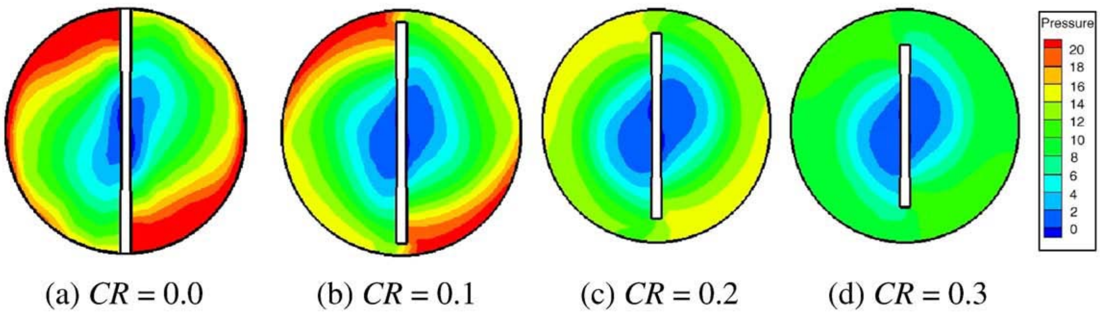

Fig. 7. Contour plots of static pressure at different clearance ratios (CR) for $y/w = 5.0$: (a) CR = 0.0, (b) CR = 0.1, (c) CR = 0.2, and (d) CR = 0.3.

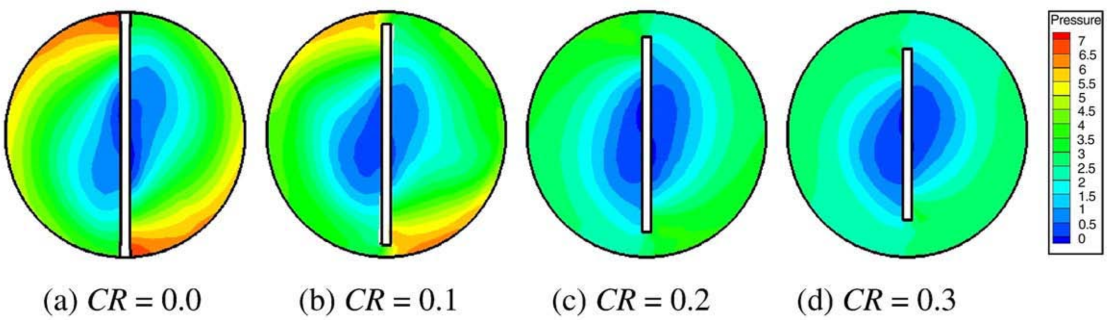

Fig. 8. Contour plots of static pressure at different clearance ratios (CR) for $y/w = 5.0$: (a) CR = 0.0, (b) CR = 0.1, (c) CR = 0.2, and (d) CR = 0.3.

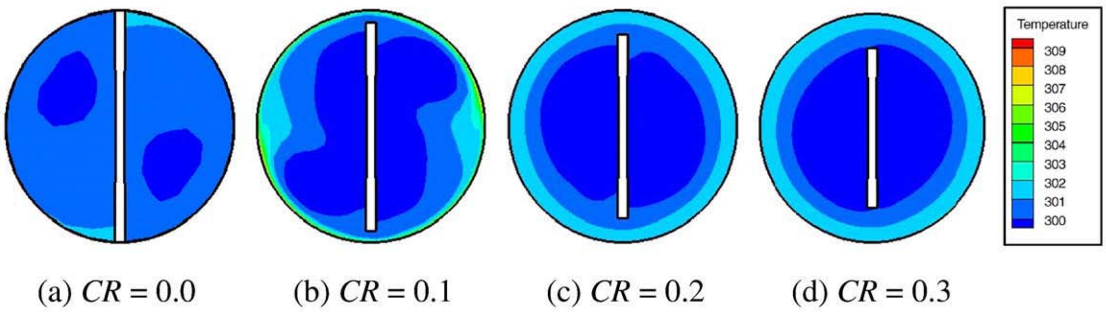

Fig. 9. Contour plots of temperature field at different clearance ratios (CR) for $y/w = 2.5$: (a) CR = 0.0, (b) CR = 0.1, (c) CR = 0.2, and (d) CR = 0.3.

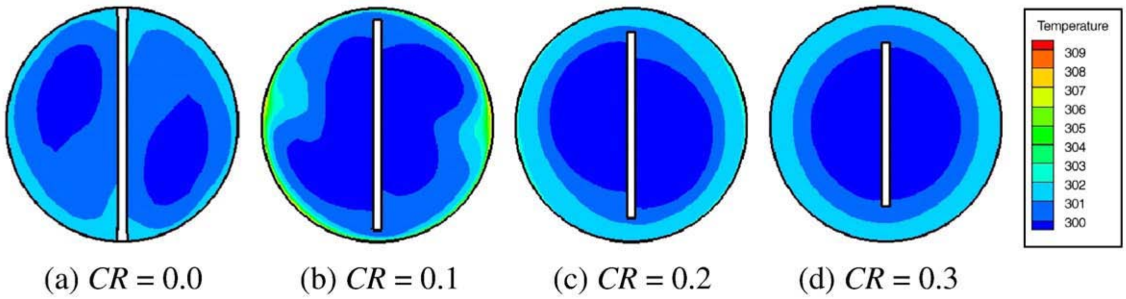

Fig. 10. Contour plots of temperature field at different clearance ratios (CR) for $y/w = 5.0$: (a) CR = 0.0, (b) CR = 0.1, (c) CR = 0.2, and (d) CR = 0.3.

absence of reversed flow by the use of the twisted tapes with larger clearance ratios, CR = 0.2 and 0.3, is responsible to poorer mixing in the tube and thus, noticeably thicker thermal boundary layers in the radial direction. On the other hand, the tight-fit twisted tapes (CR = 0) generate even stronger swirling flow than the twisted tapes with CR = 0.1, resulted in superior mixing compared to all loose-fit twisted tapes. Hence, fairly uniform temperature distribution is achieved.

4.3.5. Turbulence kinetic energy

Effect of the clearance ratios (CR) on the turbulence kinetic energy (TKE) is presented in Figs. 11(a–d) and 12(a–d). For general observation, the magnitude of TKE is high near the tube wall and also the twisted tape location where the shear stress is high [2]. An exceptional case is found only near the tube wall in the tube with the twisted tape at CR = 0.1. This may be affected by the reversed flow in the region.

4.4. Heat transfer

Effect of the tight-fit twisted tapes (CR = 0.0) and loose-fit twisted tapes (CR = 0.1, 0.2 and 0.3) on the heat transfer rate is numerically studied and presented in Fig. 13(a–b). The results for the tube fitted with all twisted tapes are also compared with those for a plain tube [15] under similar operation conditions. For both twist ratios, the heat transfer rate in terms of Nusselt numbers for twisted tape with CR = 0.1 is comparable to those for the tight-fit twisted tapes (CR = 0.0). Heat transfer rates are found to noticeably decrease with increasing clearance ratio. This is due to the fact that a system with a larger free spacing area generates a weaker swirl flow, resulting in a thicker thermal or hydrodynamic boundary layer. On the other hand, the tight-fit twisted tape or the smaller clearance ratio (CR = 0.1) provides a strong swirl flow that creates fluctuation of energy between fluid layers especially between the tape and tube wall, thus, heat can be transferred efficiently across fluid layers. The quantitative results show that, the mean heat transfer rates for the tube with twisted tape inserts for $y/w = 2.5$ with CR = 0.0, 0.1, 0.2 and 0.3 are 73.6%, 46.6%, 17.5% and 20%, respectively, higher than that for the plain tube. It should be noted that at $y/w = 2.5$, the mean heat transfer rate for the tape with CR = 0.1, is slightly lower than that for the tight-fit twisted tape (CR = 0.0) with difference around 15.6%.

4.5. Friction factor

The friction factor characteristic in a round tube fitted with twisted tape at various clearance ratios (CR) is displayed in Fig. 14(a–b). As

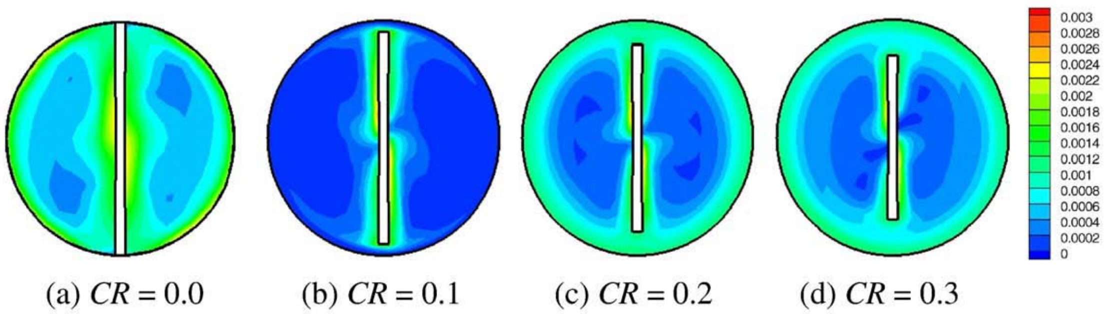

Fig. 11. Contour plots of TKE at different clearance ratios (CR) for $y/w = 2.5$: (a) CR = 0.0, (b) CR = 0.1, (c) CR = 0.2, and (d) CR = 0.3.

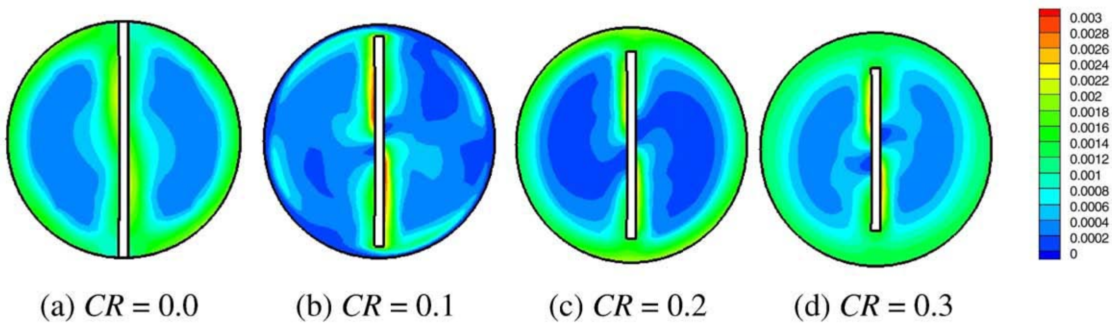

Fig. 12. Contour plots of TKE at different clearance ratios (CR) for $y/w = 5.0$: (a) CR = 0.0, (b) CR = 0.1, (c) CR = 0.2, and (d) CR = 0.3.

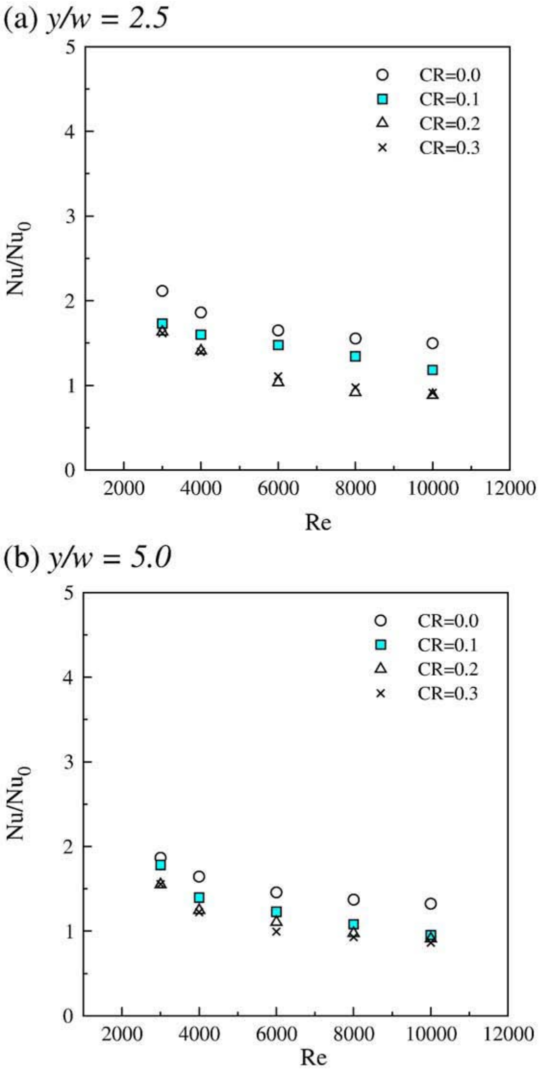

Fig. 13. Relationship between Nusselt number and Reynolds number: (a) $y/w=2.5$ and (b) $y/w=5.0$.

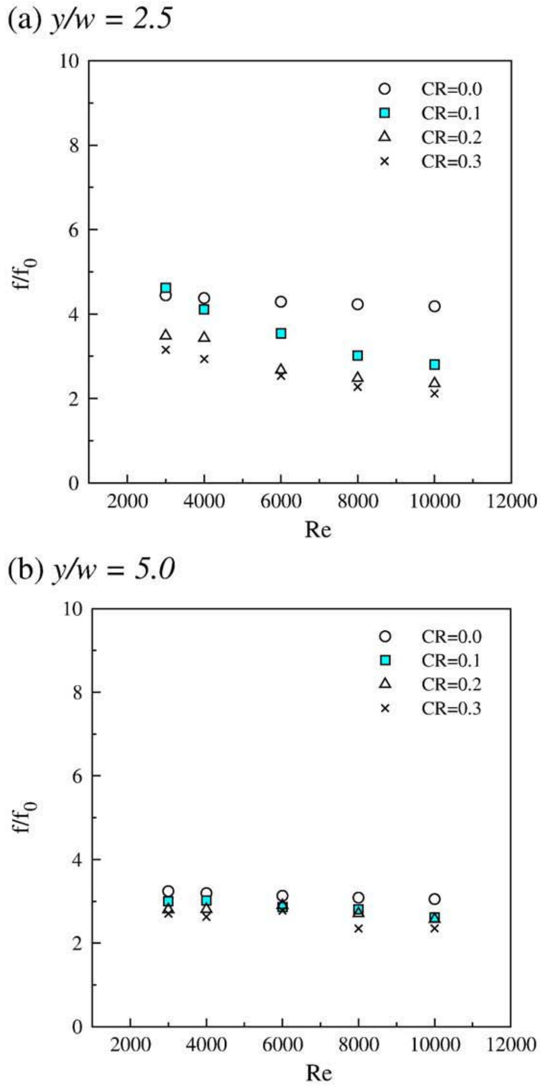

Fig. 14. Relationship between friction factor and Reynolds number: (a) $y/w=2.5$ and (b) $y/w=5.0$.

expected, friction factor decreases with increasing clearance ratio, for both twist ratios. At twist ratio, $y/w=2.5$, the friction factors in the tube with the tapes at CR = 0.0, 0.1, 0.2 and 0.3, are, respectively, around 4.18 to 4.44, 2.8 to 4.62, 2.35 to 3.49, and 2.12 to 3.15 times of that in the plain tube. However, at $y/w=5.0$, the friction factors in the tube with the tapes for various clearance ratios are just slightly different. This might be due to the low intensity of swirl flow for all tapes at the twist ratio of 5.0.

4.6. Thermal performance factor

Thermal performance factors in a tube fitted with loose-fit twisted tapes (CR = 0.1, 0.2 and 0.3) and tight-fit twisted tape (CR = 0.0) obtained using numerical simulation are depicted in Fig. 15(a–b). It is observed that the thermal performance factor tends to decrease with increasing Reynolds number for all twisted tapes. For both of twist ratios ($y/w=2.5$ and 5.0), the tight-fit twisted tapes (CR = 0.0) give the best thermal performance factors which are comparable to those provided by the loose-fit twisted tapes with the smallest clearance ratio (CR = 0.1).

5. Conclusions

The numerical analysis of heat and fluid-flows through a round tube fitted with twisted tape is carried out, with the aim to investigate the effect of tape clearance ratio (CR = c/D) on the flow, heat transfer and friction loss behaviors. A finite volume method with the standard k–ε turbulence model, the Renormalized Group (RNG) k–ε turbulence model, the standard k–ω turbulence model, and the Shear Stress Transport (SST) k–ω turbulence model, is used in the simulation. The computations show that predicted results by SST k–ω turbulence, are in good agreement with the measurements than other models. The contour plots of predicted velocity vector, static pressure, temperature, and turbulent kinetic energy (TKE) are also presented. The obtained results show that, the mean heat transfer rates for the tube with twisted tape inserts for $y/w=2.5$ with CR = 0.0, 0.1, 0.2 and 0.3 are respectively, 73.6%, 46.6%, 17.5% and 20.1% higher than that for the plain tube. The therzmal performance factor of the twisted tape is influenced by the clearance ratios (CR) and the best thermal performance factor at constant pumping power is found at clearance ratio, CR = 0.0 (tight-fit twisted tape).

Acknowledgements

The authors gratefully acknowledge the financial support by the Thailand Research Found (TRF).

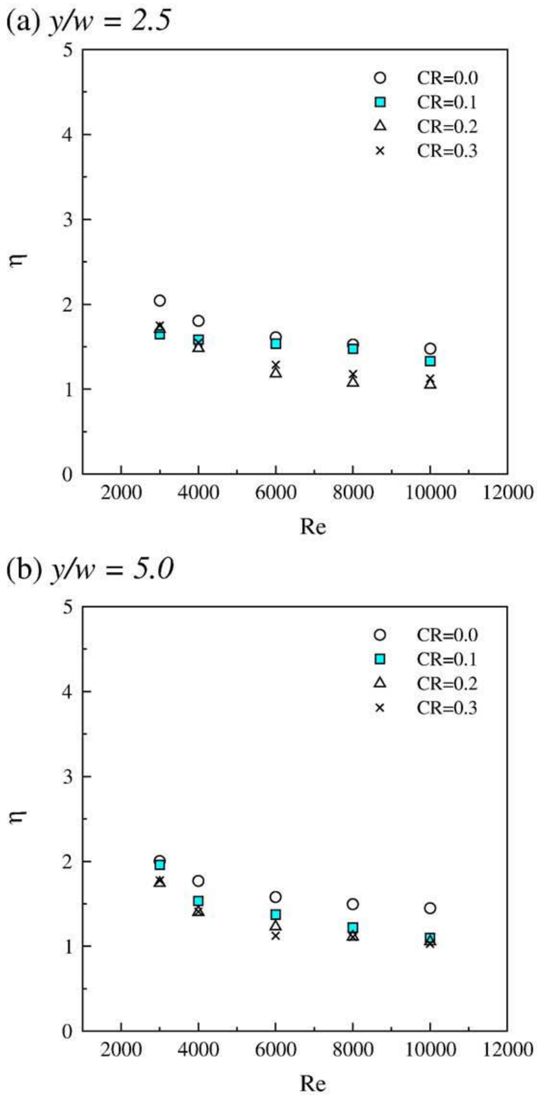

Fig. 15. Relationship between thermal performance factor and Reynolds number: (a) $y/w = 2.5$ and (b) $y/w = 5.0$.

References

[1] A.W. Date, J.R. Singham, Numerical prediction of friction and heat transfer characteristics of fully developed laminar flow in tubes containing twisted tapes, Transaction of ASME, Journal of Heat Transfer, paper no. 72-HT-17, 1972.

[2] A.W. Date, Prediction of fully developed flow in a tube containing a twisted tape, International Journal of Heat and Mass Transfer 17 (1974) 845–859.

[3] J.P. Du Plessis, Laminar flow and heat transfer in a smooth tube with a twisted-tape insert, Ph.D Thesis, Department of Mechanical Engineering, University of Stellubosch, South Africa, 1982.

[4] J.P. Du Plessis, D.G. Kroger, Friction factor prediction for fully developed laminar twisted tape flow, International Journal of Heat and Mass Transfer 27 (1984) 2095–2100.

[5] A.W. Date, S.K. Saha, Numerical prediction of laminar flow and heat transfer characteristics in a tube fitted with regularly spaced twisted-tape elements, International Journal of Heat and Fluid Flow 11 (1990) 346–354.

[6] A.W. Date, Numerical prediction of laminar flow and heat transfer in a tube with twisted-tape insert: Effects of property variations and buoyancy, Journal of Enhanced Heat Transfer 7 (2000) 217–229.

[7] S. Ray, A.W. Date, Laminar flow and heat transfer through square duct with twisted tape insert, International Journal of Heat and Fluid Flow 22 (2001) 460–472.

[8] S. Ray, A.W. Date, Friction and heat transfer characteristics of flow through square duct with twisted tape insert, International Journal of Heat and Mass Transfer 46 (2003) 889–902.

[9] P.K. Sarma, T. Subramanyam, P.S. Kishore, V. Dharma Rao, Sadik Kakac, A new method to predict convective heat transfer in a tube with twisted tape inserts for turbulent flow, International Journal of Thermal Sciences 41 (2002) 955–960.

[10] V. Zimparov, Prediction of friction factors and heat transfer coefficients for turbulent flow in corrugated tubes combined with twisted tape inserts, Part I: friction factors, International Journal of Heat and Mass Transfer 47 (2004) 589–599.

[11] V. Zimparov, Prediction of friction factors and heat transfer coefficients for turbulent flow in corrugated tubes combined with twisted tape inserts, Part II: heat transfer coefficients, International Journal of Heat and Mass Transfer 47 (2004) 385–393.

[12] Y. Kazuhisa, H. Hidetoshi, T. Saburo, S. Chikahiro, Numerical simulation on heat transfer enhancement in twisted-tape-inserted tubes, Journal of Enhanced Heat Transfer 11 (2004) 379–389.

[13] M. Rahimi, S.R. Shabanian, A.A. Alsairafi, Experimental and CFD studies on heat transfer and friction factor characteristics of a tube equipped with modified twisted tape inserts, Chemical Engineering and Processing: Process Intensification 48 (3) (2009) 762–770.

[14] R.M. Manglik, A.E. Bergles, Heat transfer and pressure drop correlations for twisted-tape inserts in isothermal tubes, part II: transition and turbulent flows, transaction ASME, Journal of Heat Transfer 115 (1993) 890–896.

[15] F.P. Incropera, P.D. Witt, T.L. Bergman, A.S. Lavine, Fundamentals of Heat and Mass Transfer, John-Wiley & Sons, 2006.


Volume 36 Number 7
August 2009
ISSN 0735-1933
ELSEVIER
International Communications in
HEAT and MASS TRANSFER
Editor-in-Chief
W.J. MINKOWYCZ
Editors
A.R. BALAKRISHNAN, P. CHENG, R. GREIF, C.P. GRIGOROPOULOS, E. HAHNE,
A.I. LEONTIEV, O.G. MARTYNENKO, J.W. ROSE, J. TAINE, H. YOSHIDA
Available online at
ScienceDirect
www.sciencedirect.com

International Communications in Heat and Mass Transfer 36 (2009) 698–704

Contents lists available at ScienceDirect

International Communications in Heat and Mass Transfer

journal homepage: www.elsevier.com/locate/ichmt

Compound heat transfer enhancement of a dimpled tube with a twisted tape swirl generator ☆

Chinaruk Thianpong [a,*], Petpices Eiamsa-ard [a], Khwanchit Wongcharee [b], Smith Eiamsa-ard [c]

[a] Department of Mechanical Engineering, Faculty of Engineering, King Mongkut's Institute of Technology Ladkrabang, Bangkok 10520, Thailand
[b] Department of Chemical Engineering, Faculty of Engineering, Mahanakorn University of Technology, Bangkok 10530, Thailand
[c] Department of Mechanical Engineering, Faculty of Engineering, Mahanakorn University of Technology, Bangkok 10530, Thailand

ARTICLE INFO

Available online 3 May 2009

Keywords:
Compound heat transfer
Friction factor
Dimpled tube
Twisted tape

ABSTRACT

Friction and compound heat transfer behaviors in a dimpled tube fitted with a twisted tape swirl generator are investigated experimentally using air as working fluid. The effects of the pitch and twist ratio on the average heat transfer coefficient and the pressure loss are determined in a circular tube with the fully developed flow for the Reynolds number in the range of 12,000 to 44,000. The experiments are performed using two dimpled tubes with different pitch ratios of dimpled surfaces ($PR = 0.7$ and 1.0) and three twisted tapes with three different twist ratios ($y/w = 3$, 5, and 7). Experiments using plain tube and dimpled tube acting alone are also carried out for comparison. The experimental results reveal that both heat transfer coefficient and friction factor in the dimpled tube fitted with the twisted tape, are higher than those in the dimple tube acting alone and plain tube. It is also found that the heat transfer coefficient and friction factor in the combined devices increase as the pitch ratio (PR) and twist ratio (y/w) decrease. In addition, an empirical correlation based on the experimental results of the present study is sufficiently accurate for prediction the heat transfer (Nu) and friction factor (f) behaviors.

1. Introduction

A large portion of energy being consumed in industry processes and the energy resources are depleting at an alarming rate. Energy conservation is therefore, become an important issue. In many areas of the industries, using of high-performance heat exchanger is one of the promising energy-saving manners.

The high-performance heat exchangers can be obtained by utilization of heat transfer enhancement techniques. In general, heat transfer enhancement creates one or more combinations of the following conditions that are favorable for the increase in heat transfer rate with an undesirable increase in friction: (1) interruption of boundary layer development and rising degree of turbulence, (2) increase in heat transfer area, and (3) generating of swirling and/or secondary flows [1]. Several enhancement techniques have been introduced, for example, treated surfaces, rough surfaces, swirling flow devices, coiled tubes, and surface tension devices [2]. Numerous works have revealed that dimpled tube and twisted tape are effective devices for enhancing heat transfer rate. Here, some of the related works are described as follows. Rabas et al. [3] reported the influence of roughness shape and spacing on the performance of three-dimensional helically dimpled tubes. Chen et al. [4] performed an experimental work to study the heat transfer coefficient, friction factor and enhancement index characteristics in a dimpled tube at different depth/pitch of dimples. Their results showed that the heat transfer rates were enhanced from 25% to 137% at constant Reynolds number, and 15% to 84% at constant pumping power. Vicente et al. [5] reported the effects of the three-dimensional helically dimpled tubes (dimpled height, $h/d = 0.08$ to 0.12 and helical pitch, $p/d = 0.65$ to 1.1) on the heat transfer and isothermal friction in turbulent flow region. Vicente et al. [6] also conducted an experimental work to determine the heat transfer and friction characteristics in dimpled tubes in laminar and transition flow regions using water and ethylene glycol as working fluids. They observed that laminar flow heat transfer through horizontal dimpled tubes is produced in mixed convection, where Nusselt number depends on both the natural convection and the entry region.

Insertion of twisted tape is one of the effective methods to increase heat transfer coefficient with relatively small pressure drop penalty. Twisted tape has been used to create swirling flows that modify the near wall velocity profile due to the various vorticity distributions in the vortex core. The fluid mixing between the tube core and the near wall region is enhanced because of the swirl induce tangential flow velocity component [1]. The twisted tape and other heat transfer enhancement devices were also utilized simultaneously to gain better results compared to that by a single device. This approach is known as compound enhancement [2]. Al-Fahed et al. [7] carried out an experimental work to study the heat transfer coefficients and friction

☆ Communicated by W.J. Minkowycz.

* Corresponding author.
E-mail addresses: cthianpong@yahoo.com (C. Thianpong), smith@mut.ac.th (S. Eiamsa-ard).

0735-1933/$ – see front matter © 2009 Elsevier Ltd. All rights reserved.
doi:10.1016/j.icheatmasstransfer.2009.03.026

Nomenclature

A	surface area of test tube, m^2
C_p	specific heat at constant pressure, J/kg K
D	tube diameter, m
e	depth of dimple, m
f	friction factor
h	convective heat transfer coefficient, W/m^2 K
k	thermal conductivity, W/m K
L	length of tube, m
$\dot{m}$	mass flow rate, kg/s
Nu	Nusselt number
p	pitch of dimple, m
PR	pitch ratio = p/D
Pr	Prandtl number
Q	heat transfer rate, W
Re	Reynolds number
T	temperature, °C
U	mean velocity in tube, m/s or overall heat transfer coefficient, W/m^2 K
w	width of tape, m
y	twist length of tape, m
y/w	twist ratio
δ	tape thickness, mm
ρ	density, kg/m^3
μ	dynamic viscosity, kg/m s

Subscripts

ave	average
b	bulk
c	cold
h	hot
H	hydraulic
i	inner
in	inlet
o	outer
out	outlet
w	water

factors in a microfin tube fitted with twisted tape for three different twist/width ratios under laminar flow region. Liao and Xin [8] conducted an experimental study to determine the heat transfer and friction characteristics in tubes with three-dimensional internal extended surfaces combined with a twisted tape using various working fluids (water, ethylene glycol, and ISO VG46 turbine). Zimparov [9] combined the single start spirally corrugated tubes with the twisted tape inserts for their heat transfer enhancement. Pramanik and Saha [10] investigated the heat transfer and friction loss for laminar flow with viscous oil through rectangular and square ducts with internal transverse rib turbulators on two opposite surfaces of the ducts and fitted with twisted tapes. The tapes used were full length, short length, and regularly spaced types. They found that the transverse ribs in combination with full-length twisted tapes performed better than either ribs or twisted tapes acting alone. The pressure drop and compound heat transfer characteristics of a converging–diverging tube with evenly spaced twisted tapes were considered by Mengna et al. [11]. Their results showed that the heat transfer rates were 0.85 to 1.21 times of those in a plain tube and 1.07 to 1.15 times of those in a converging–diverging tube without twisted tape inserts. Promvonge and Eiamsa-ard [12] investigated the heat transfer, friction factor and thermal enhancement characteristics in a tube with combined conical-ring turbulator and twisted tape. Recently, Promvonge [1] reported the influences of wire coils in conjunction with twisted tapes on the heat transfer and friction factor in a uniform heat-flux tube.

The advantages of the dimpled tube, twisted tape and compound heat transfer enhancement, shown in literature review above, motivate us to investigate heat transfer enhancement by using the dimpled tube together with the twisted tape as compound enhancing device. In the present work, the effects of pitch and twist ratios on the heat transfer coefficient and pressure loss characteristics in the fully developed turbulent flow of a dimpled tube with a twisted tape insert are examined. The Reynolds numbers are ranged from 12,000 to 44,000 with hot/cold water as working fluid. The experimental results of the heat transfer enhancement and pressure loss as well as the empirical correlation for Nusselt number and friction factor are presented.

2. Test section

The experimental work was conducted to reach a more practical look at the influences of a dimpled tube in conjunction with a twisted tape for both heat transfer enhancement and pressure loss in a concentric tube heat exchanger. Two dimpled tubes of different pitch ratios, in conjunction with three twisted tape inserts of different twisted ratios were used for comparison with the standard plain tube and also the dimpled tube acting alone. A schematic drawing of a concentric tube heat exchanger and the dimpled tube combined with a twisted tape is given in Figs. 1 and 2 while the details of the test conditions are also presented in Table 1. The dimpled surfaces were arranged in staggered line for two pitch ratios of $PR = p/D = 0.7$ and 1.0. The dimpled diameter (d) and dimpled depth (e) were kept at a constant value of 3 mm and 2 mm, respectively. The dimpled tubes were made of copper with length of 1500 mm and installed in a concentric tube heat exchanger as an inner tube using hot water as working fluid. The twisted tapes were made of straight aluminum tape with thickness (δ) of 0.5 mm, width (w) of 22 mm, and twist ratios $y/w = 3$, 5 and 7. The twist ratio is defined herein as the ratio of two twist length (y, 180°) to the tape width (w). Details of the experimental set-up and the method for conducting the experiment are similar as reported in earlier paper [13].

3. Data deduction

The average Nusselt number and the friction factor are based on the inner diameter of the test tube. Heat absorbed by the cold water in the annulus, Q_c can be written by

$$Q_c = \dot{m}_c C_{p,w}\left(T_{c,out} - T_{c,in}\right) \tag{1}$$

where $\dot{m}_c$ is the mass flow rate of cold water; $C_{p,w}$ is the specific heat of water; $T_{c,in}$ and $T_{c,out}$ are the inlet and outlet cold water temperatures, respectively. The heat supplied from the hot water, Q_h can be determined by

$$Q_h = \dot{m}_h C_{p,w}\left(T_{h,out} - T_{h,in}\right) \tag{2}$$

where $\dot{m}_c$ is the hot water mass flow rate; $T_{h,in}$ and $T_{h,out}$ are the inlet and outlet hot water temperatures, respectively. The heat supplied by the hot fluid into the test tube is found to be 2 to 4% higher than the heat absorbed by the cold fluid for thermal equilibrium due to convection and radiation heat losses from the test section to surroundings. Thus, the average value of heat transfer rate, supplied and absorbed by both fluids, is taken for internal convective heat transfer coefficient calculation.

$$Q_{ave} = \frac{Q_c + Q_h}{2} \tag{3}$$

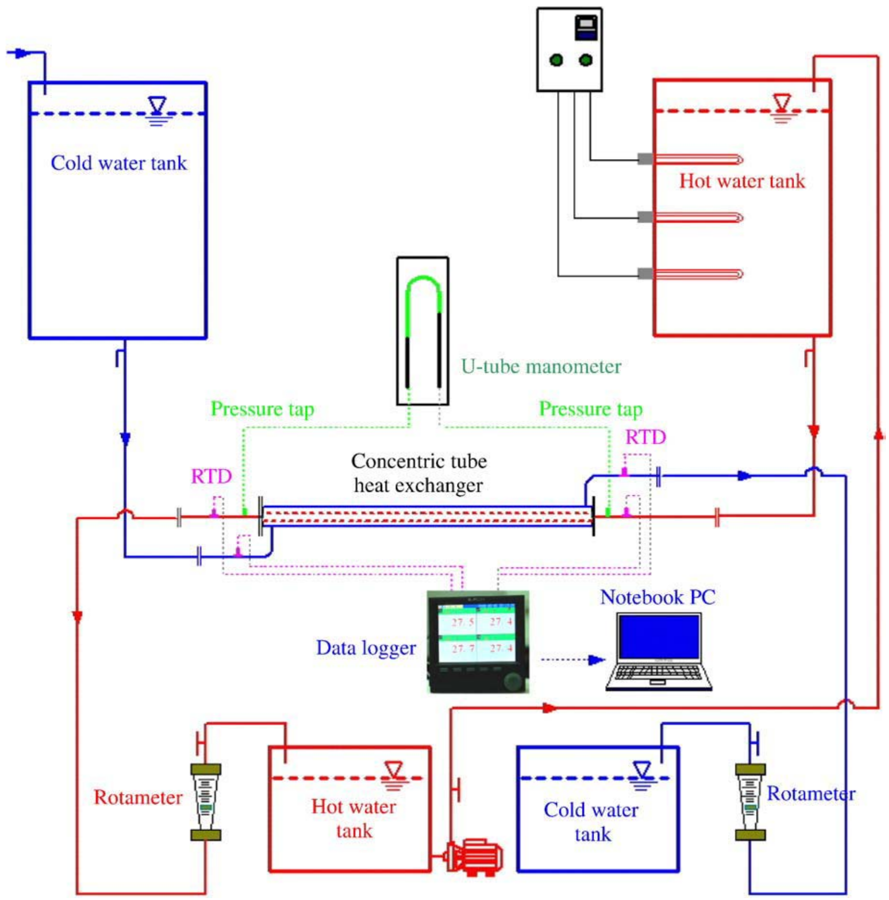

Fig. 1. Schematic diagram of the test apparatus.

For fluid flows in a concentric tube heat exchanger, the heat transfer coefficient (h_i) is calculated from

$$Q_{ave} = UA_i\Delta T_{LMTD} \quad (4)$$

where

$$A_i = \pi D_i L$$

The tube side heat transfer coefficient is then determined (by neglecting of the thermal resistance in the copper tube wall) using

$$\frac{1}{U} = \frac{1}{h_i} + \frac{1}{h_o} \quad (5)$$

where the annulus side heat transfer coefficient (h_o) is estimated by using the correlation of Dittus–Boelter [14];

$$\mathrm{Nu}_o = \frac{h_o D_H}{k} = 0.023\mathrm{Re}^{0.8}\mathrm{Pr}^{0.3} \quad (6)$$

then,

$$h_o = \frac{k}{D_H}\mathrm{Nu}_o$$

where

$$D_H = D_o - D_i$$

thus,

$$\mathrm{Nu} = \frac{h_i D_i}{k}$$

The local thermal conductivity (k) of the fluid is calculated from the fluid properties at the local mean bulk fluid temperature. The

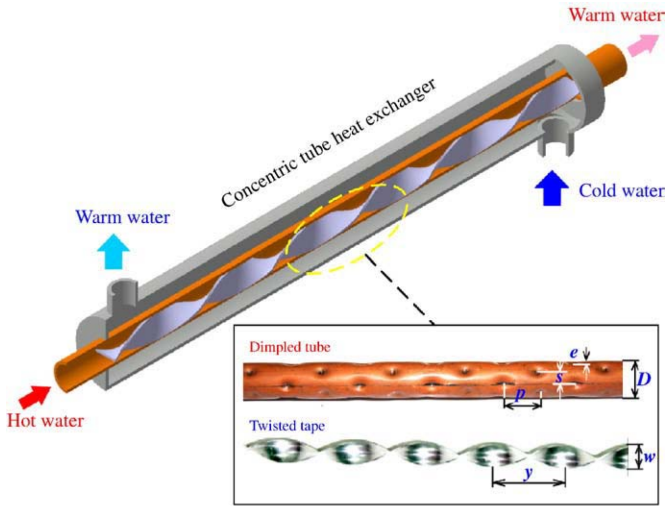

Fig. 2. Dimpled tube and twisted tape.

Table 1
Detail of test conditions.

Test condition	
(a) Reynolds number, (*Re*)	12,000 to 44,000
(b) Working fluid	Cold/hot water
(c) Inlet cold water temperature, ($T_{c,i}$)	28 °C
(d) Inlet hot water temperature, ($T_{h,i}$)	70 °C
Concentric tube heat exchanger	
(a) Inner tube diameter (plain tube), (D_i)	22 mm
(b) Outer tube diameter, (D_o)	38 mm
(c) Test tube length	1500 mm
(d) Material of inner tube	Copper
(e) Material of outer tube	Stainless steel
Dimpled tube	
(a) Dimpled outer tube diameter, (*D*)	22.2 mm
(b) Dimpled tube thickness, (*t*)	0.8 mm
(c) Dimpled pitch length, (*p*)	15.5 and 22.2 mm
(d) Pitch ratio, $PR = p/D$	0.7 and 1.0
(e) Dimpled diameter (*d*)	3 mm
(f) Dimpled depth (*e*)	2 mm
Twisted tape	
(a) Tape width, (*w*)	22 mm
(b) Tape pitch length, (*y*, 180°)	66, 110, and 154 mm
(c) Twist ratio, (y/w)	3, 5, and 7
(d) Tape thickness, (δ)	0.5 mm
(e) Materials	Aluminium

Reynolds number is based on the different flow rate at the inlet of the test section.

$$\mathrm{Re} = \rho U D / \mu \tag{7}$$

where μ is the dynamic viscosity of the working fluid.

Friction factor (f) can be written as:

$$f = \frac{\Delta P}{\left(\frac{L}{D}\right)\left(\rho \frac{U^2}{2}\right)} \tag{8}$$

which U is mean velocity in the tube. All of thermo-physical properties of the water are determined at the overall bulk water temperature.

4. Experimental results and discussion

In this section, the following results are, respectively presented, the validity test of plain tube, the effect of combination of the dimpled tube with the twisted tape, the effect of pitch ratio, and the effect of twist ratio. Finally, the empirical correlations for Nusselt number and friction factor are developed.

4.1. Validity tests of the plain tube

Prior to the experiments using the dimpled tube combined with the twisted tape, the Nusselt number and the friction factor in a plain tube were measured. The experimental data were, then compared with the results given by the well known correlations under a similar condition, in order to evaluate the validity of the plain tube. The comparisons for Nusselt number and friction factor are shown in Fig. 3(a) and (b), respectively. Obviously, the experimental data are in good agreement with existing correlations, which are Dittus–Boelter correlation, Petukhov correlation, and Blasius correlation. It is noted that the Nusselt number differs by up 7% from the Dittus–Boelter correlation [14] while the friction factor differs by up 18% from the Blasius correlation. In addition, the experimental results of the present study are correlated with Nusselt number and friction factor as follows,

$$\mathrm{Nu} = 0.049\mathrm{Re}^{0.706}\mathrm{Pr}^{0.4} \tag{9}$$

$$f = 0.718\mathrm{Re}^{-0.309} \tag{10}$$

4.2. Effect of combined dimpled tube and twisted tape

Experimental results of the Nusselt number (*Nu*) and friction factor (f) characteristics in dimpled tubes combined with a twisted tape ($y/w = 3$) are presented in Fig. 4(a) and (b), respectively. The Nusselt number and friction factor of the plain tube or the dimple tube acting alone are also plotted for comparison. The data show that the Nusselt number (*therefore, the heat transfer coefficient*) increases with increasing Reynolds number for the conventional turbulent tube flow. Depending on Reynolds number (*Re*), the Nusselt number of the dimpled tube with the twisted tape insert is 15 to 56% higher than that in the dimpled tube acting alone and 66 to 303% higher than that in the plain tube (Fig. 4(a)). It is noted that the increasing Nusselt number in the dimpled tube in common with a twisted tape is caused by the generating of pressure gradient along the radial direction, and this leads to redeveloping of thermal/hydrodynamic boundary layer. The higher increase of the Nusselt number in this style of both turbulence and swirl flows is a consequence of the higher reduction of boundary layer thickness and increase of resultant velocity. Fig. 4(b) shows the influence of a dimpled tube combined with a twisted tape on pressure loss, which indicates the friction in a heat exchanger. The mean increase of friction factor in the combined devices is up to 2.12 times of that in the dimple tube acting alone and 5.58 times of that in the plain tube.

4.3. Effect of pitch ratio

The influence of the pitch ratios ($PR = 0.7$ and 1.0) on the Nusselt number in a dimpled tube in common with a twisted tape is shown in Fig. 4(a). As expected, the Nusselt number in the dimple tube

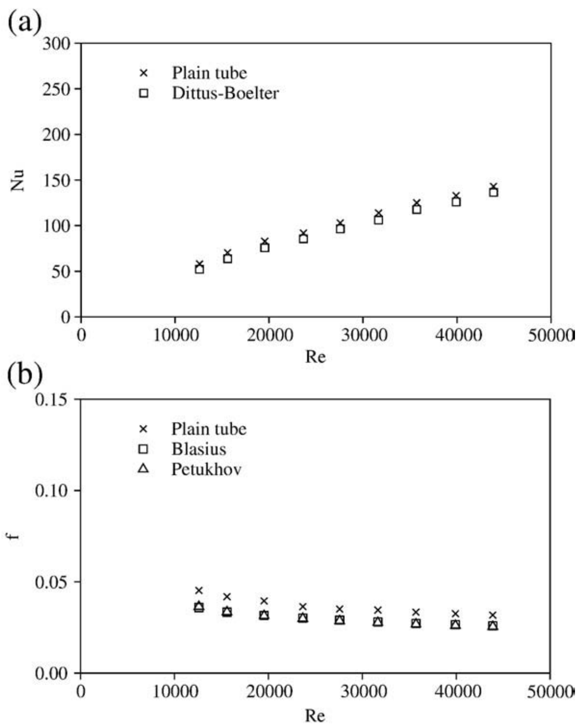

Fig. 3. Comparisons of experimental data and empirical correlations of the plain tube for (a) Nusselt number and (b) friction factor.

combined with twisted tape for $PR = 0.7$ is considerably higher than those for higher pitch ratio ($PR = 1.0$). The mean increase in Nusselt number of the dimpled tube with the twisted tape is in a range of 2.15 to 3.03 times for $PR = 0.7$ and 1.66 to 1.92 times for $PR = 1.0$, in comparison with that of the plain tube. This is due to the fact that, twisted tape with smaller pitch ratio ($PR = 0.7$), is more effective for interruption of development of the thermal/hydrodynamic boundary layer of the fluid flow and increase the degree of turbulence intensity than that with larger pitch ratio ($PR = 1.0$). Fig. 4(b) presents the effect of the pitch ratio (PR) on the friction factor in a dimpled tube combined with twisted tape. It is found that, the friction factor in the tube with the smaller pitch ratio ($PR = 0.7$) is higher than that with the larger pitch ratio ($PR = 1.0$) around 6 to 14.8%. This is a result of the higher flow mixing effect for the dimpled tube with the lower pitch ratio, leading to greater turbulence intensity.

4.4. Effect of twist ratio

Fig. 5(a–b) shows the effect of the twist ratios ($y/w = 3$, 5 and 7) on the Nusselt number of a dimpled tube in common with a twisted tape insert. The Nusselt number increases as the Reynolds number increases, and this trend is the most obvious for the smallest twist

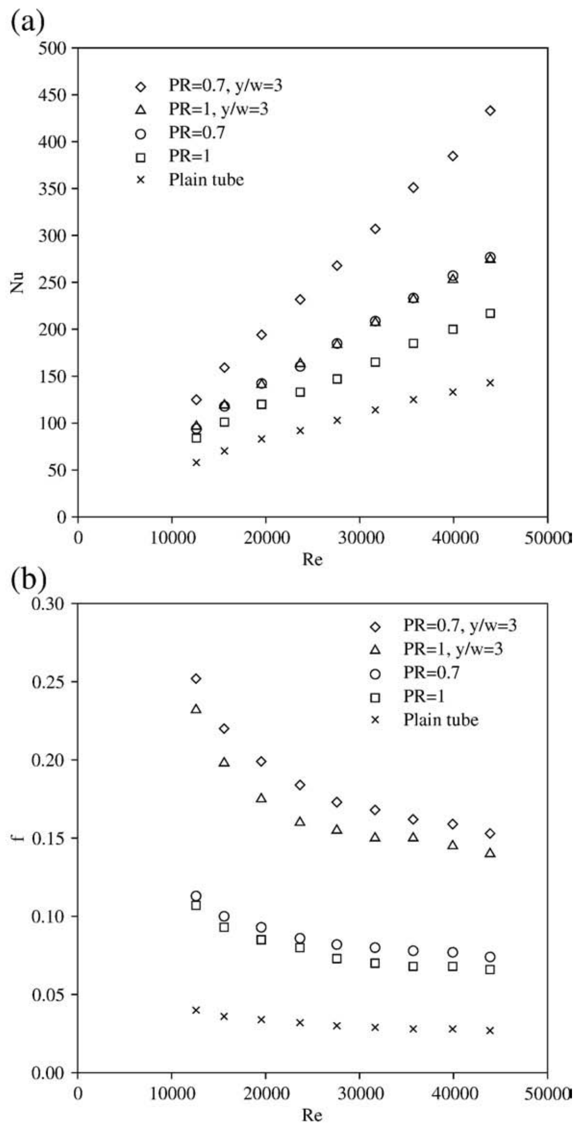

Fig. 4. Effects of dimpled tube in common with twisted tape on (a) Nusselt number and (b) friction factor.

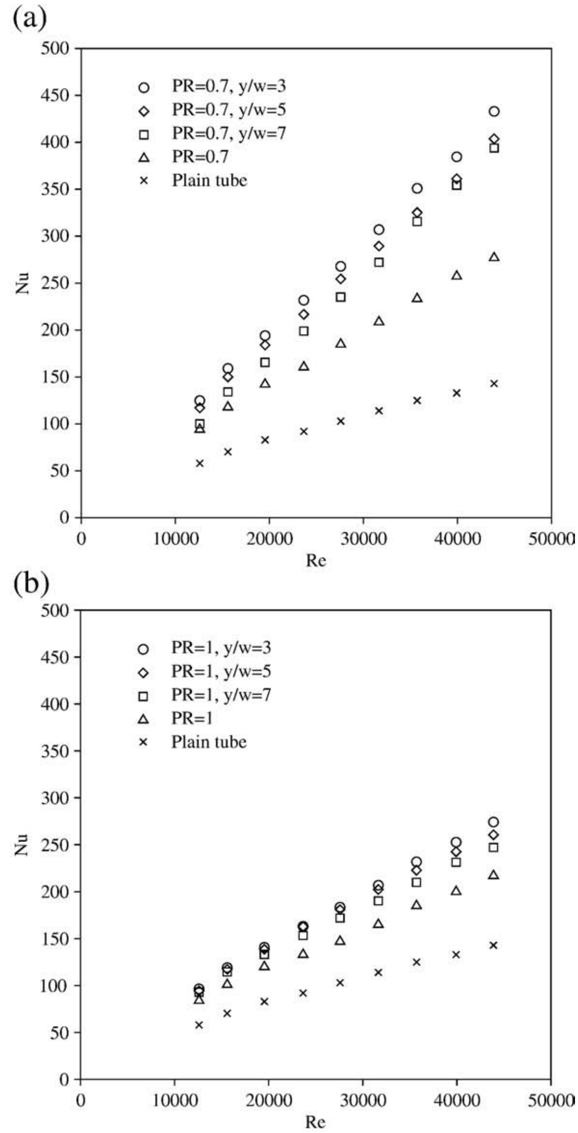

Fig. 5. Effect of twist ratio on heat transfer enhancement for (a) $PR = 0.7$ and (b) $PR = 1.0$.

ratio ($y/w = 3$). At the same Reynolds number, the Nusselt number increases with the decreasing twist ratio. The reasons are that, turbulence intensity and also residence time increase with the decreasing twist ratio. Fig. 6(a–b) shows the effect of twist ratio (y/w) on the friction factor in a dimpled tube combined with a twisted tape. It is obvious that the friction factor of the dimpled tube in conjunction with a twisted tape increases as twist ratio (y/w) decreases. Approximately, the friction factors for employing the dimpled tube combined with a twisted tape at the smallest twist ratio ($y/w = 3$) are found to be 9.7% and 18.3% over those at the twist ratio, $y/w = 5$ and 7, respectively.

From the experimental results, the Nusselt number and friction factor in a dimpled tube acting alone are function of Reynolds number (Re) and pitch ratio (PR), while those in the dimpled tube fitted with a twisted tape are also function of twist ratio (y/w). The empirical correlations developed for a dimpled tube acting alone are expressed as

$$\mathrm{Nu} = 0.04\mathrm{Re}^{0.76}(PR)^{-0.59}\mathrm{Pr}^{0.3} \tag{11}$$

$$f = 2.69\mathrm{Re}^{-0.35}(PR)^{-0.29} \tag{12}$$

The empirical correlations developed for a dimpled tube in common with a twisted tape are expressed as

$$\mathrm{Nu} = 0.014\mathrm{Re}^{0.9}(PR)^{-0.93}(y/w)^{-0.12}\mathrm{Pr}^{0.3} \quad (13)$$

$$f = 9.1\mathrm{Re}^{-0.37}(PR)^{-0.11}(y/w)^{-0.2} \quad (14)$$

The fitted values of the Nusselt number and friction factor from Eqs. (11)–(14) are compared with the experimental values and presented in Fig. 7(a–b). The fitted values from the above equations are found agree well with the experimental data within ±10% for both Nusselt number and friction factor.

5. Conclusions

An experimental study of fully developed turbulent flow in a dimpled tube in conjunction with a twisted tape has been performed. The influences of the pitch ratio and twist ratio on the heat transfer rate and friction factor characteristics have also been investigated. A dimpled tube in common with a twisted tape has significant effects on the heat transfer enhancement and friction factor. The heat transfer and friction factor are increase with decreasing both of pitch ratio (PR) and twist ratio (y/w). Depending on the pitch ratio and twist ratio, the heat transfer rate and friction factor in the dimpled tube with twisted tape, are respectively 1.66 to 3.03 and 5 to 6.31 times of those in the plain tube. The empirical correlations for the Nusselt number and the friction factor based on the present experimental data are also presented.

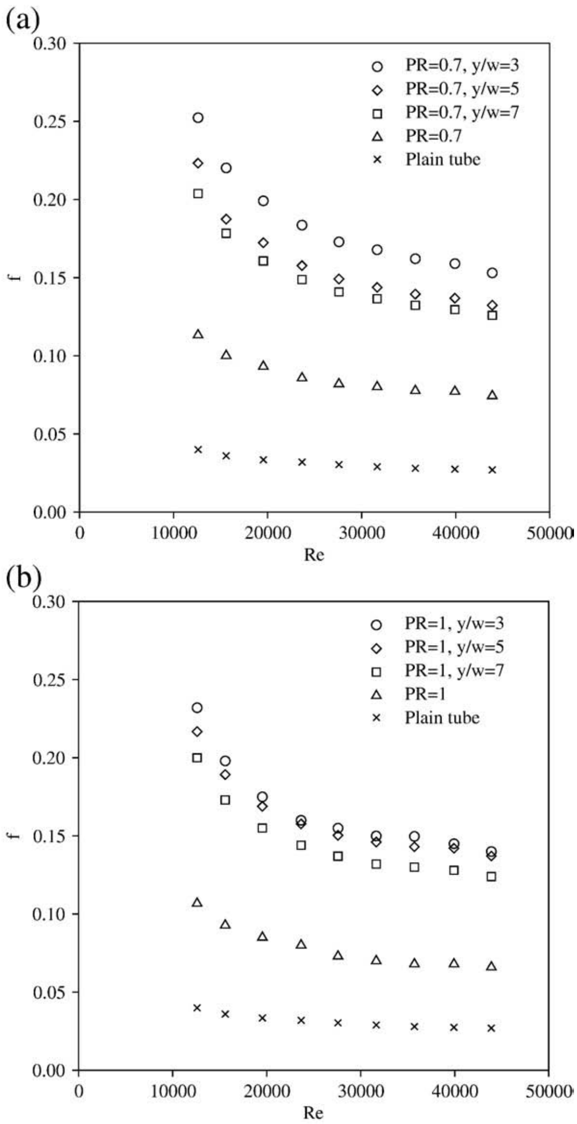

Fig. 6. Effect of twist ratio on friction factor for (a) $PR = 0.7$ and (b) $PR = 1.0$.

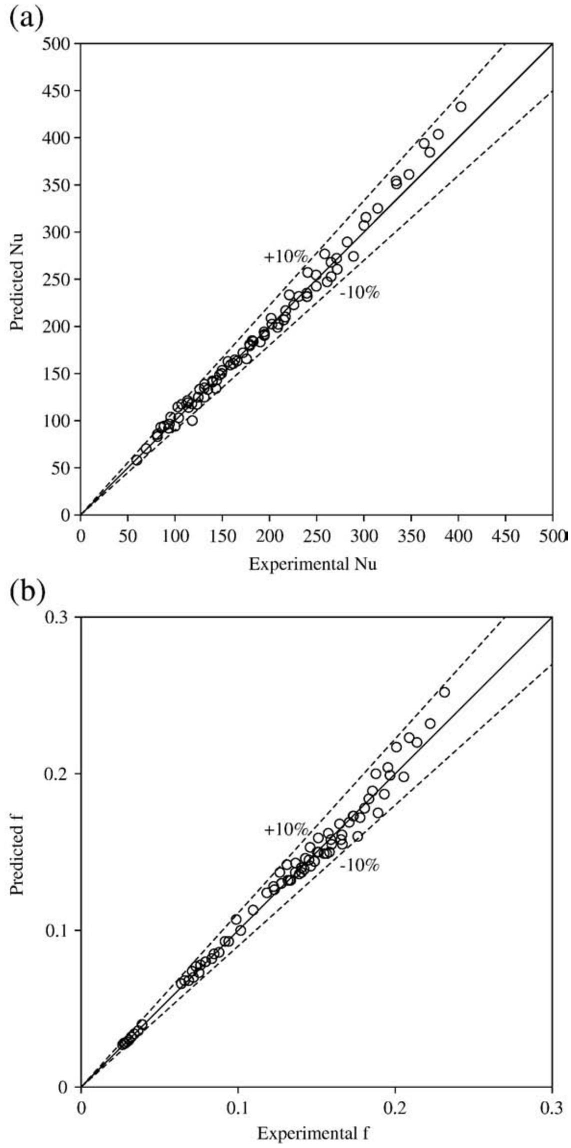

Fig. 7. Comparison between experimental and predicted for (a) Nusselt number and (b) friction factor.

Acknowledgement

The authors would like to gratefully acknowledge the Thailand Research Fund (TRF) for the financial support of this research.

References

[1] P. Promvonge, Thermal augmentation in circular tube with twisted tape and wire coil turbulators, Energy Conversion and Management 49 (2008) 2949–2955.
[2] A.E. Bergles, ExHFT for fourth generation heat transfer technology, Experimental Thermal and Fluid Science 26 (2002) 335–344.

[3] T.J. Rabas, R.L. Webb, P. Thors, N.K. Kim, Influence of roughness shape and spacing on the performance of three dimensional helically dimpled tubes, Journal of Enhanced Heat Transfer 1 (1993) 53–64.
[4] J. Chen, H. Müller-Steinhagen, G.G. Duffy, Heat transfer enhancement in dimpled tubes, Applied Thermal Engineering 21 (2001) 535–547.
[5] P.G. Vicente, A. Garcıa, A. Viedma, Heat transfer and pressure drop for low Reynolds turbulent flow in helically dimpled tubes, International Journal of Heat and Mass Transfer 45 (2002) 543–553.
[6] P.G. Vicente, A. Garcıa, A. Viedma, Experimental study of mixed convection and pressure drop in helically dimpled tubes for laminar and transition flow, International Journal of Heat and Mass Transfer 45 (2002) 5091–5105.
[7] S. Al-Fahed, L.M. Chamra, W. Chakroun, Pressure drop and heat transfer comparison for both microfin tube and twisted-tape inserts in laminar flow, Experimental Thermal and Fluid Science 18 (1999) 323–333.
[8] Q. Liao, M.D. Xin, Augmentation of convective heat transfer inside tubes with three-dimensional internal extended surfaces and twisted-tape inserts, Chemical Engineering Journal 78 (2000) 95–105.
[9] V. Zimparov, Enhancement of heat transfer by a combination of three-start spirally corrugated tubes with a twisted tape, International Journal Heat and Mass Transfer 44 (2001) 551–574.
[10] D. Pramanik, S.K. Saha, Thermohydraulics of laminar flow through rectangular and square ducts with transverse ribs and twisted tapes, Journal of Heat Transfer, Transactions of ASME 128 (2006) 1070–1080.
[11] H. Mengna, D. Xianhe, H. Kuo, L. Zhiwu, Compound heat transfer enhancement of a converging–diverging tube with evenly spaced twisted-tapes, Chinese Journal of Chemical Engineering 15 (2007) 814–820.
[12] P. Promvonge, S. Eiamsa-ard, Heat transfer behaviors in a tube with combined conical-ring and twisted-tape insert, International Communications in Heat and Mass Transfer 34 (2007) 849–859.
[13] S. Eiamsa-ard, S. Pethkool, C. Thianpong, P. Promvonge, Turbulent flow heat transfer and pressure loss in a double pipe heat exchanger with louvered strip inserts, International Communications in Heat and Mass Transfer 35 (2007) 120–129.
[14] F.P. Incropera, P.D. Witt, T.L. Bergman, A.S. Lavine, Fundamentals of Heat and Mass Transfer, John-Wiley & Sons, 2006.

Proceedings of the 14th International Heat Transfer Conference
IHTC14
August 7-13, 2010, Washington D.C., USA

IHTC14-22500

HEAT TRANSFER ENHANCEMENT IN A TUBE FITTED WITH TWISTED TAPE SWIRL GENERATOR

Smith Eiamsa-ard
Mahanakorn University of Technology
Bangkok, Thailand

Panida Seemawute
Mahanakorn University of Technology
Bangkok, Thailand

Khwanchit Wongcharee
Mahanakorn University of Technology
Bangkok, Thailand

ABSTRACT

Flow friction, heat transfer and thermal performance characteristics in a tube fitted with peripherally-cut twisted tape (*PT*) have been experimentally investigated. The twist ratio (*y/W*) of twisted tape was varied from 3 to 5 while the depth of peripheral cut ratio (*d/W*) and the width of peripheral cut ratio (*w/W*) were both kept constant at 0.22. The experiments were conducted for the Reynolds number ranging from 5100 to 19,700, using water as a working fluid. The plain tube and the tube equipped with the typical twisted tape (*TT*) with three different twist ratios (*y/W* = 3, 4 and 5) were also tested for comparison. The obtained results reveal that the use of *PT* enhances Nusselt number up to 211% and 138% compared to those of the plain tube and the tube with *TT*, respectively. It is also found that heat transfer rate increases with decreasing twist ratio. Additionally, the performance evaluation to assess the real benefits in using the *PT* as heat transfer enhancer has also been determined.

TWISTED INSERT OVERVIEWS

The technology of heat transfer enhancement (HTE) has gained a lot of attention over the past several decades. HTE finds applications mainly in the design of more compact heat exchanger at various engineering applications, especially refrigeration, automotive and chemical process industries. Insertion of twisted tapes in a tube provides a simple passive technique for enhancing the convective heat transfer by introducing swirl into the bulk flow and disrupting the thermal boundary layer at the tube surface due to the repeated changes in the twisted tape geometry. The major advantages of heat transfer enhancement by inserting twisted-tape are the low assets and easy setting up.

Many research works have been performed to investigate the effect of geometries of twisted-tapes on heat transfer and friction within heat exchanger by both experimental and numerical approaches. Date and Saha [1] numerically predicted the friction and heat transfer characteristics for laminar flow in a circular tube fitted with regularly spaced twisted-tape elements which were connected by thin circular rods. Hong and Bergles [2] experimentally studied the effect of the twisted-tape insert on heat transfer rate and pressure drop in laminar flow under uniform heat flux. Lepina and Bergles [3] developed correlations of the heat transfer for turbulent flow. Kumar and Prasad [4] investigated the effect of twisted tape insert on the heat transfer, friction factor and thermal performance factor characteristics in solar water heaters. Rahimi et al. [5] examined the influences of jagged, notched, and perforated twisted-tapes on the heat transfer, friction factor and thermal performance characteristics in a circular tube. Their results showed that the thermal performance of the jagged twisted tape was higher than those of the other tape inserts. Naphon [6] studied the influence of the twist ratios of twisted tape on the heat transfer and pressure drop in a horizontal double pipe heat exchanger. It was found that the tape with the smallest twist ratio provides the highest heat transfer enhancement and pressure loss. Eiamsa-ard et al. [7-9] determined the effect of regularly spaced twisted tape elements, short-length twisted tape and loose-fit twisted tape on heat transfer enhancement in a heat exchanger. Chang et al. [10] presented the influence of the serrated twisted tape, consisting of repeated ribs as turbulators on the heat transfer, friction factor and thermal performance factor. Their findings were that the serrated tape induced friction factor as high as 80 times of the plain tube, this consequently led to the lower thermal performance factor compared to those provided by the typical one. Eiamsa-ard et al. [11] considered the effect of the delta-winglet twisted tape on the heat transfer enhancement in a heat exchanger tube under uniform heat flux condition. Chang et al. [12] and Eiamsa-ard et al. [13-14] also reported the results of heat transfer enhancement using single and twin twisted tapes. Chang et al. [12] proved that the twin and triple tapes provided higher thermal performance factor than the typical/single tape. Effect of the twin twisted tapes with counter/co-swirling flow on the thermal performance factor was investigated by Eiamsa-ard et al. [14]. Chang et al. [15] invented broken twisted tape which provided a higher thermal performance factor than the serrated twisted tape and the typical tape from the open literature. Chang et al. [16] also investigated the effect of a spiky twisted tape two-phase flow structures, pressure drops and thermal-fluid performance behaviors in single and two phase flows (air-water). Jaisankar et al. [17-20] presented the effects of helical twisted tape with space at the trailing edge and left-right twisted tape on the heat transfer and friction factor characteristics for solar water heater system.

Regarding to the literature mentioned above, the performance of twisted tape insert as heat transfer enhancement device, is strongly dependent on the tape geometry. The goal of the present work is to investigate the effect of the modified twisted tape in form of the peripherally-cut twisted tape (*PT*) on the enhanced heat transfer. The peripheral cut on the *PT* was anticipated to give the additional turbulence in the vicinity of the tube wall. The experiments were performed using the *PTs* with three different twist ratios (y/W = 3, 4, and 5). The depth of peripheral cut ratio (d/W) and the width of peripheral cut ratio (w/W) of all *PTs* were both kept constant at 0.22. All of the experiments were carried out at the same inlet conditions with the Reynolds number, based on the tube diameter, ranging from of 5100 to 19,700. In addition, the empirical correlations for Nusselt number, friction factor and thermal performance factor have also been developed.

PERIPHERALLY-CUT TWISTED TAPE (PT)

All of the twisted tapes used in the present work were made of aluminium sheet with thickness (δ) of 0.8 mm. and tape length (l) of 1000 mm. The tape width (W) of peripherally-cut twisted tape (*PT)* was 18 mm while that of typical twisted tape (*TT*) was 19 mm. The *TT* was initially fabricated then peripherally cut to form the *PT*. The geometries of the *PT* and the *TT* are demonstrated in Fig. 1. In the experiments, the twisted tapes (*TT* and *PT*) with three different twist ratios (y/W = 3, 4 and 5) were tested. For the *PTs*, the depth and width of the peripheral cut were kept constant at d = 4 mm (d/W = 0.22) and w = 4 mm (w/W = 0.22). Regarding to the Fig.1, the twist ratio "y/W" is defined as the ratio of the twist length (y, 180°/twist length) to the tape width (W).

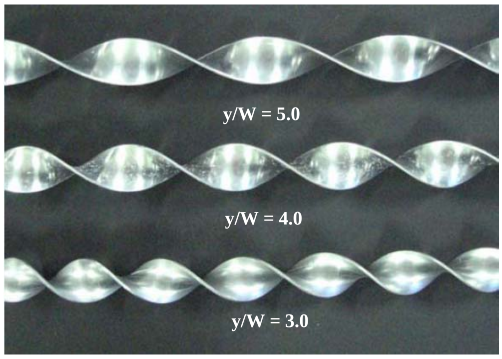

(a)

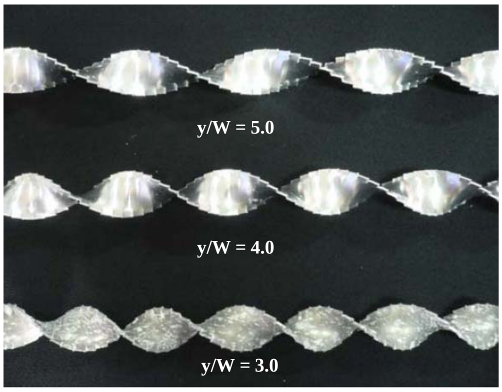

(b)

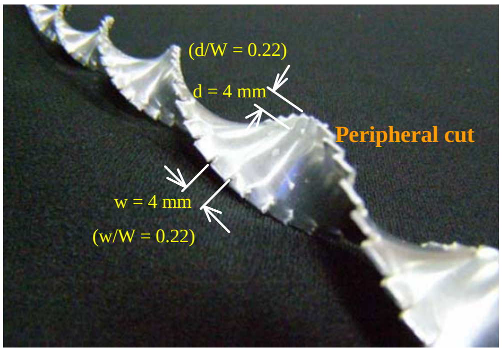

(c)

Fig. 1 Photographs of twisted tapes (a) typical twisted tape (TT), (b) peripherally-cut twisted tapes (PT) and (c) dimensions of PT tape

EXPERIMENTAL SET-UP AND PROCEDURE

The experiments were carried out using an experimental facility shown in Fig. 2. The test tube was made of copper with inner diameter of 19.5 mm (D), outer diameter of 21 mm (D_o), wall thickness of 1.5 mm (t), and length of 1000 mm (L). In the experiments, the typical or peripherally-cut twisted tape (*TT* or *PT*) was inserted into a test tube. A rather long tube provided a sufficient contact surface between a tape and a tube wall for the firm attachment of the tape to the tube without the need of any extra fitting. During the test, the tube was heated by continually winding flexible electrical wire. The electrical output power was controlled via a variac transformer to obtain a constant wall heat flux along the entire length of the test section. The outer surface of the test tube was well insulated to minimize convective heat leak to surroundings. Moreover, necessary precautions were taken to prevent leakages from the system. In the experiment, the heat transfer losses from the test tube are around 3 to 5% of the total heat input ($Q = IV$). The inlet and outlet temperatures of the water were measured using multi-channel temperature measurement unit in conjunction with the resistance temperature detectors (RTDs). Fifteen thermocouples were tapped on the local wall of the tube to measure the circumferential temperature variation, which was found to be negligible. The average local wall temperature was determined by means of calculations based on the reading of Copper-Constantan thermocouples.

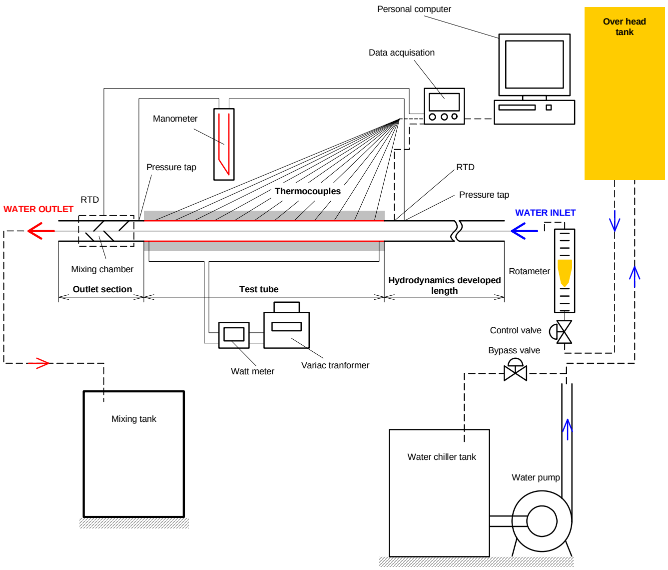

Fig. 2 Schematic diagram of experimental heat transfer apparatus

During the test, the water from a reservoir tank was discharged through a rotameter to measure the volumetric flow rate and then forced to the heat transfer test section. For each test run, it was necessary to record the data of temperature, volumetric flow rate and pressure drop of the bulk water at steady state condition in which the inlet water temperature was maintained at 27^{o}C. The characteristics of the flow friction and the Reynolds numbers were based on bulk temperature. The average Nusselt numbers were calculated and discussed where all fluid properties were determined at the overall bulk average temperature. The Reynolds number of the cold water was varied from 5100 to 19,700. The uncertainties of axial velocity, pressure and temperature measurements estimated based on ANSI/ASME [21] are found to be within ±7%, ±5% and ±0.5%, respectively. In addition, the uncertainties of non-dimensional parameters are within ±5% for Reynolds number, ±10% for Nusselt number and ±12% for friction.

HEAT TRANSFER AND FRICTION MEASUREMENTS

In experiments, water is used as a working fluid and flowed through a test tube under uniform wall heat flux condition. The rate of heat absorbed by water at steady state is assumed to be equal to the rate of convective heat transfer within the test section which can be expressed as:

$$Q_{water} = Q_{conv} \tag{1}$$

Then the heat transferred from the water flow can be drawn as,

$$Q_{water} = MC_p(T_{out} - T_{in}) \tag{2}$$

The heat transferred from the tube wall by convection can be written as,

$$Q_{conv} = hA\left|\tilde{T}_w - \left(\frac{T_{out} + T_{in}}{2}\right)\right| \tag{3}$$

where T_{out} is the outlet temperature of water flow, T_{in} is the inlet water temperature, $\tilde{T}_w$ is a mean wall temperature calculated from the local wall temperatures along the test tube wall and A is the total surface area of the inner tube wall, which can be expressed as:

$$A = \pi DL \tag{4}$$

where D and L are the inner diameter and length of the test tube, respectively. Combining equations (2) and (3) results in the equation for average heat transfer coefficient (h) as

$$h = \frac{MC_p(T_{out} - T_{in})}{A\left|\tilde{T}_w - \left(\frac{T_{out} + T_{in}}{2}\right)\right|} \tag{5}$$

Then the average Nusselt number can be calculated from

$$Nu = \frac{hD}{k} \tag{6}$$

where k is the thermal conductivity of the fluid.

Friction factor of the tube with or without twisted tape can be calculated using pressure loss (ΔP) across the test length (L) via the following equation

$$f = \frac{1}{2}\frac{\Delta P}{L}\frac{D}{\rho U^2} \tag{7}$$

where ρ is the density at the average bulk temperature, and U is the average velocity based on the inner diameter. The Nusselt number, Prantl number, Reynolds number, and all of thermo-physical properties of the fluid were calculated of the basis of water properties corresponding to the bulk fluid temperature (T_b). The Reynolds number based on the total flow rate at the inlet of the test section is expressed as:

$$Re = \rho UD / \mu \tag{8}$$

where μ is the dynamic viscosity of the working fluid.

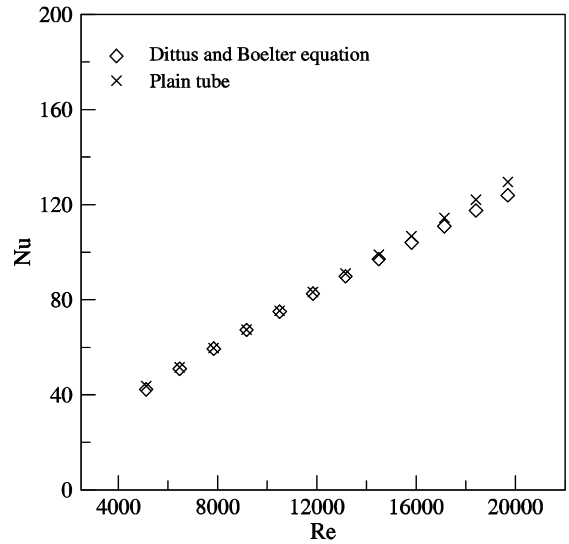

Fig. 3 Comparison of present experimental plain tube data with those calculated from Dittus-Boelter correlation [22]

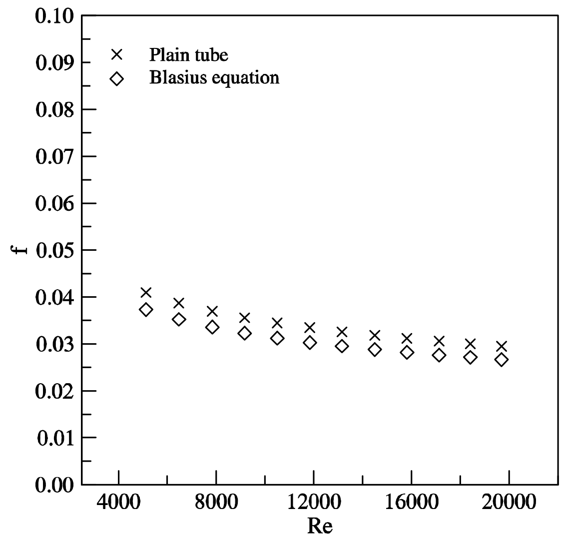

Fig. 4 Comparison of present experimental plain tube data with those calculated from Blasius correlation [22]

EXPERIMENTAL RESULTS

The heat transfer enhancement, pressure drop and thermal performance factor characteristics in terms of Nusselt number (*Nu*), friction factor (*f*) and thermal performance (η) are respectively reported and discussed in this section.

Validation of the plain tube

In order to evaluate the experimental facility reliability, it is necessary to verify present plain tube data with those calculated from the well known correlations including, Dittus-Boelter for Nusselt number and Blasius [22] for friction factor. The comparisons for Nusselt number and friction factor are shown in Figs. 3 and 4, respectively. It is found that the present data are in good agreement with those obtained from Dittus-Boelter and Blasius correlations. In addition, the empirical correlations for Nusselt number and friction factor have also been derived using the experimental data. The resultant correlations are shown in equations (9) and (10). The developed correlations provide fairly accurate data within ±2% to ±4% error limits.

$$Nu = 0.03277Re^{0.742}\,Pr^{0.4} \tag{9}$$

$$f = 0.6165Re^{0.317} \tag{10}$$

Heat transfer results

Influence of twist ratio. The relationship between Nusselt number and Reynolds number in a uniform heat flux tube fitted with the typical and peripherally-cut twisted tapes (*TT* and *PT*) of various twist ratios (*y/W* = 3, 4 and 5) is depicted in Fig. 5. Apparently, the presence of *TT* or *PT* in the enhanced tube leads heat transfer improvement with respect to the plain tube, due to the better fluid mixing assisted by the tape. For all cases, Nusselt number increases with Reynolds number. At the given Reynolds number, Nusselt number increases as twist ratio (*y/W*) decreases. This is a consequence of the stronger turbulent intensity generated by the twisted tape with a smaller twist ratio. Over the range studied, the mean Nusselt numbers for the tube fitted with *PTs* with *y/W* = 3, 4 and 5 are respectively, 111%, 93% and 79% over that for the plain tube, and 32%, 36%, and 38% over that for the tube fitted with *TT* at the same twist ratio.

*Influence of peripherally-cut twisted tape (PT)***.** From experimental results, it can be observed that at the same twist ratio the heat transfer enhancement given by peripherally-cut twisted tape (*PT*) is superior to that offered by the typical twisted tape (*TT*) as presented in Fig. 5. Evidently, the heat transfer rates of the *PTs* are found to be higher than those of the *TTs* by around 28 to 36%. This indicates that the thermal boundary layer disruption caused by the *PTs* is more efficient than that associated by the typical one.

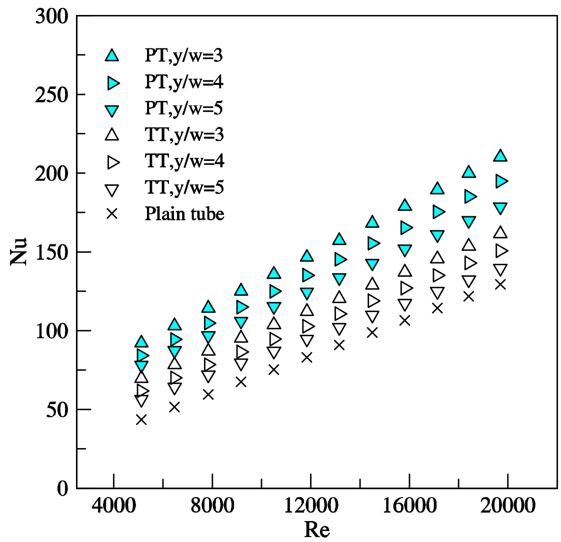

Fig. 5 Relationship between Nusselt number and Reynolds number

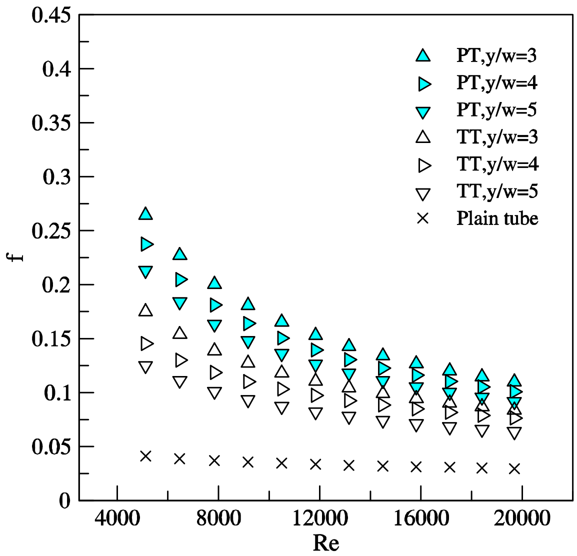

Fig. 6 Relationship between friction factor and Reynolds number

Friction factor results

Influence of twist ratio. Effects of the twist ratios (y/W = 3, 4 and 5) for both peripherally-cut twisted tape (*PT*) and typical twisted tape (*TT*) on friction factor are depicted in Fig. 6. In the present studies, the pressure drop is presented in term of friction loss. As expected, the friction factor in tube with twisted tape insert is significantly higher than that in the tube without twisted tape insert. Moreover, the results reveal that the use of the tape with a smaller twist ratio leads to the higher friction factor due to the stronger swirl intensity. This results in a higher tangential contact between the flow and the tube surface. Therefore, the twisted tape with the smallest twist ratio (y/W = 3) possesses a maximum friction factor. Regarding to the obtained results, the mean friction factors in the tube with *PTs* at y/W = 3, 4 and 5 are respectively 4, 5.8 and 5.2 times of the plain tube.

Influence of peripherally-cut twisted tape (PT). As shown in Fig. 6, the peripherally-cut twisted tape (*PT*) induces considerably higher friction factors than the typical twisted tape (*TT*), under the similar conditions. It can be quantified that the friction factors in the tube with *PTs* at y/W = 3, 4 and 5, are approximately 1.38, 1.44 and 1.54 times of those the tube with *TTs* at the same twist ratio. With the help of experimental data, the following empirical Nusselt numbrt and friction factor relationships were derived for the tube fitted with peripherally-cut twisted tape. Figs. 7 and 8 show comparisons between the present experimental and predicted data. As seen, results of the predicted data agree well with present experimental data within ±6% for the Nusselt number, and within ±5% for the friction factor.

$$Nu = 0.306\, Re^{0.625}\, Pr^{0.4} \left(y / w\right)^{-0.318} \tag{11}$$

$$f = 93.189\, Re^{-0.639} \left(y / w\right)^{-0.377} \tag{12}$$

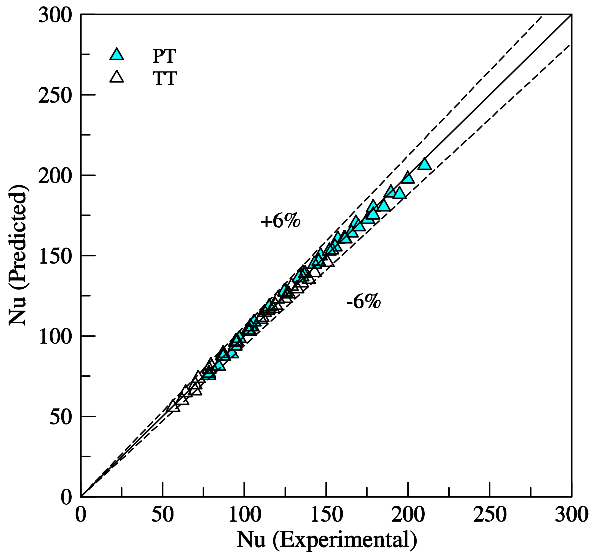

Fig. 7 Comparison of present experimental data with the predicted data obtained from Eq. (11) for peripherally-cut twisted tape

Thermal performance factor results

The thermal performance factor for a constant pumping power is a useful parameter for determining the effectiveness of heat transfer enhancement of the heat transfer promoter in comparison with the plain tube [23]. The relationship of the volumetric flow rate and the pressure loss under constant pumping power of each tube can be drawn as

$$(\dot{V}\Delta P)_p = (\dot{V}\Delta P)_t \tag{13}$$

Using the Darcy equation for pressure drop and Reynolds number, equation (13) can be rewritten as

$$(f\, Re^3)_p = (f\, Re^3)_t \tag{14}$$

The thermal performance factor (η) at constant pumping power can be written as:

$$\eta = (Nu_t/Nu_p)/(f_t/f_p)^{1/3} \tag{13}$$

The thermal performance factor at the same pumping power shown in equation (13), in which the pressure drop is presented in the form of friction factor, is usually used to evaluate the potential of the twisted tape for practical applications. The factor above unity indicates a more efficient heat transfer by the use of twisted tape with respect to the use of plain tube while the factor below unity indicates a worse heat transfer. In addition, most of the studies on heat transfer enhancement, the thermal performance factor $((Nu_t/Nu_p)/(f_t/f_p)^{1/3})$ is usually plotted against the Reynolds number. From the results shown in Fig. 9, the thermal performance factor found to be increased with decreasing Reynolds number and twist ratio (y/W). The peripherally-cut tape (*PT*) with the smallest twist ratio (y/W = 3) provides the thermal performance higher than those offers by the tapes with y/W = 4 and 5. It can be quantified that the *PTs* with y/W = 3, 4 and 5 give the maximum thermal performance factors at 1.14, 1.08 and 1.04, respectively. In addition, the *PT*s provided the mean thermal performance higher than those proposed by the *TTs* around 15%.

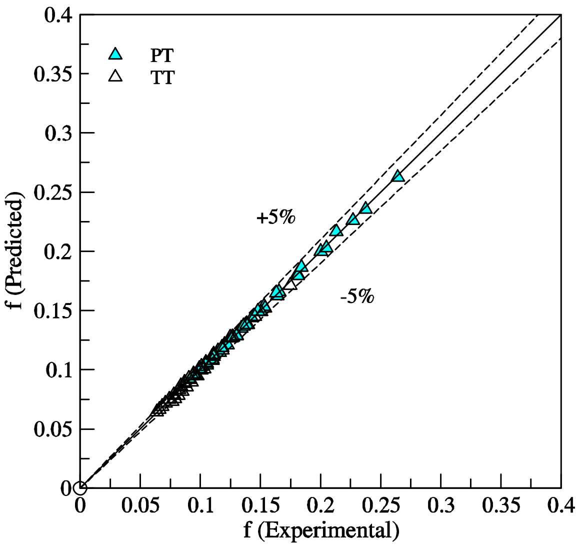

Fig. 8 Comparison of present experimental data with the predicted data obtained from Eq. (12) for peripherally-cut twisted tape

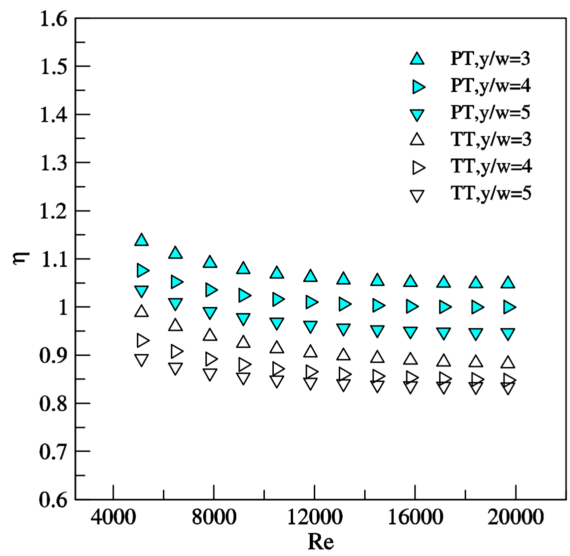

Fig. 9 Relationship between thermal performance and Reynolds number

CONCLUSIONS

The present paper describes the improvement of heat transfer rate in a heat exchanger by installing the peripherally-cut twisted tapes (*PTs*). The obtained results demonstrate that the *PTs* with twist ratios of y/W = 3, 4 and 5 provide the mean Nusselt number up to 111%, 93% and 79% over the plain tube and 32%, 36%, and 38% over the tube fitted with the typical twisted tapes (*TTs*) at the same twist ratios, for Reynolds number ranging from 5100 to 19,700. This can be explained by the fact that the *PTs* provide a better mixing than a typical twisted tape. Besides the common swirl flow, it is presumed that the additional turbulence of fluid in the vicinity of the tube wall is also generated by the *PTs*, removing the viscous sub-layer near tube wall and thus leading to a superior heat transfer improvement. The thermal performances of the peripherally-cut twisted tapes (*PTs*) are 12-18% higher than those of typical twisted tapes (*TTs*). In the present work *PTs* consistently provide higher thermal performance factor than the *TTs*, this indicates the better performance of the *PTs* with respect to that of the *TTs*. Over the range studied, the maximum thermal performance (η) of 1.14 is found by the use of the *PT* with twist ratio of 3 at the lowest Reynolds number of 5100. In the other word, the *PT* enhances heat transfer rate up to 14% above that for the plain tube, at the identical pumping power.

ACKNOWLEDGEMENTS

The authors would like to gratefully acknowledge the Thailand Research Fund (TRF) and Thailand Toray Science Foundation was founded (TTSF) for the financial support of this research.

NOMENCLATURE

A	=	heat transfer surface area, m^2
C_p	=	specific heat of fluid, J kg^{-1} K^{-1}
d	=	peripherally-tape depth, m
D	=	inside diameter of the test tube, m
f	=	friction factor $=\Delta P/((L/D)(\rho U^2/2))$, dimensionless
h	=	heat transfer coefficient, W m^{-2} K^{-1}
I	=	current, A
k	=	thermal conductivity of fluid, W m^{-1} K^{-1}
L	=	length of the test section, m
M	=	mass flow rate, kg s^{-1}
Nu	=	Nusselt number = hD/k, dimensionless
P	=	pressure of flow in stationary tube, Pa
ΔP	=	pressure drop, Pa
Pr	=	Prandtl number = $\mu C_p/k$, dimensionless
Q	=	heat transfer rate, W
Re	=	Reynolds number = $\rho UD/\mu$, dimensionless
t	=	thickness of the test tube, m
T	=	temperature, K
$\tilde{T}$	=	average temperature, K
U	=	average axial flow velocity, m s^{-1}
V	=	voltage, V
w	=	peripherally-tape width, m
W	=	twisted tape width, m
y	=	twisted tape pitch, m

Greek Symbols

ρ	=	fluid density, kg m^{-3}
δ	=	twisted tape thickness, m

μ = fluid dynamic viscosity, kg s^{-1} m^{-1}
η = thermal performance factor, dimensionless

Subscripts
b = bulk
conv = convection
in = inlet
out = outlet
p = plain
t = twisted tape
w = wall

Abbreviations
PT = peripherally-cut twisted tape
TT = typical twisted tape

REFERENCES

[1] Date, A.W. and Saha, S.K., 1990, "Numerical prediction of laminar flow and heat transfer in a tube fitted with regularly spaced twisted-tape elements," International Journal of Heat Fluid Flow, **11**, pp. 346-354.

[2] Hong, S.W. and Bergles, A.E., 1976, "Augmentation of laminar flow heat transfer in tubes by means of twisted-tape inserts," Interim Report Iowa State Univ. of Science and Technology, Ames. Heat Transfer Lab.

[3] Lepina, R.F. and Bergles, A.E., 1969, "Heat transfer and pressure drop in tape-generated swirl flow of single-phase water," Transaction of ASME, Journal of Heat Transfer, **91**, pp. 434-442.

[4] Kumar, A and Prasad, B.N., 2000, "Investigation of twisted tape inserted solar water heaters-heat transfer, friction factor and thermal performance results," Renewable Energy, **19**, pp. 379-398.

[5] Rahimi, M., Shabanian, S.R., and Alsairafi, A.A., 2009, "Experimental and CFD studies on heat transfer and friction factor characteristics of a tube equipped with modified twisted tape inserts," Chemical Engineering and Processing **48**, pp. 762-770.

[6] Naphon, P., 2006, "Heat transfer and pressure drop in the horizontal double pipes with and without twisted tape insert," International Communications in Heat and Mass Transfer **33**, pp. 166-175.

[7] Eiamsa-ard, S., Thianpong, C., and Promvonge, P., 2006, "Experimental investigation of heat transfer and flow friction in a circular tube fitted with regularly spaced twisted tape elements," International Communications in Heat and Mass Transfer **33**, pp. 1225-1233.

[8] Eiamsa-ard, S., Thianpong, C., Eiamsa-ard, P., and Promvonge, P., 2009, "Convective heat transfer in a circular tube with short-length twisted tape insert," International Communications in Heat and Mass Transfer **36**, pp. 365-371.

[9] Eiamsa-ard, S., Wongcharee, K., and Sripattanapipat, S., 2009, "3-D Numerical simulation of swirling flow and convective heat transfer in a circular tube induced by means of loose-fit twisted tapes," International Communications in Heat and Mass Transfer **36**, pp. 947-955.

[10] Chang, S.W., Jan, Y.J., and Liou, J.S., 2007, "Turbulent heat transfer and pressure drop in tube fitted with serrated twisted-tape," International Journal Thermal Science **46**, pp. 506-518.

[11] Eiamsa-ard, S., Wongcharee, K., Eiamsa-ard, P., and Thianpong, C., 2010, "Heat transfer enhancement in a tube using delta-winglet twisted tape inserts," Applied Thermal Engineering, **30**, pp. 310-318.

[12] Chang, S.W., Yu, K.W., and Lu, M.H., 2005, "Heat transfer in tubes fitted with single, twin and triple twisted tapes," International Journal Experimental Heat Transfer **18**, pp. 279-294.

[13] Eiamsa-ard, S., Thianpong, C., Eiamsa-ard, P., and Promvonge, P., 2010, "Thermal characteristics in a heat exchanger tube fitted with dual twisted tape elements in tandem," International Communications in Heat and Mass Transfer, **37**, pp. 39-46.

[14] Eiamsa-ard, S., Thianpong, C., and Eiamsa-ard, P., 2010, "Turbulent heat transfer enhancement by counter/co-swirling flow in a tube fitted with twin twisted tapes," Experimental Thermal and Fluid Science, **34**, pp. 53-62.

[15] Chang, S.W., Yang, T.L., and Liou, J.S., 2007, "Heat transfer and pressure drop in tube with broken twisted tape insert," Experimental Thermal and Fluid Science **32**, pp. 489-501.

[16] Chang, S.W., Lees, A.W., and Chang, H.T., 2009, "Influence of spiky twisted tape insert on thermal fluid performances of tubular air-water bubbly flow," International Journal of Thermal Sciences, **48**, pp. 2341-2354.

[17] Jaisankar, S., Radhakrishnan, T.K., and Sheeba, K.N., 2009, "Experimental studies on heat transfer and friction factor characteristics of forced circulation solar water heater system fitted with helical twisted tapes," Solar Energy, **83**, pp.1943-1952.

[18] Jaisankar, S., Radhakrishnan, T.K., and Sheeba, K.N., 2009, "Studies on heat transfer and friction factor characteristics of thermosyphon solar water heating system with helical twisted tapes," Energy **34**, pp. 1054-1064.

[19] Jaisankar, S., Radhakrishnan, T.K., and Sheeba, K.N., 2009, "Experimental studies on heat transfer and friction factor characteristics of thermosyphon solar water heater system fitted with spacer at the trailing edge of twisted tapes," Applied Thermal Engineering **29**, pp. 1224-1231.

[20] Jaisankar, S., Radhakrishnan, T.K., Sheeba, K.N., and Suresh, S., 2009, "Experimental investigation of heat transfer and friction factor characteristics of thermosyphon solar water heater system fitted with spacer at the trailing edge of left-right twisted tapes," Energy Conversion and Management **50**, pp. 2638-2649.

[21] ANSI/ASME, 1986, *Measurement uncertainty*, PTC 19, 1-1985. Part I.

[22] Incropera, F.P., Witt, P.D., Bergman, T.L., and Lavine, A.S., 2006, *Fundamentals of Heat and Mass Transfer*, John-Wiley & Sons.

[23] Yakut, K., Sahin, B., and Canbazoglu, S., 2004, "Performance and flow-induced vibration characteristics for conical-ring turbulators," Applied Energy **79**, pp. 65-76.